



UIT

THE ARCTIC
UNIVERSITY
OF NORWAY

Faculty of Health Sciences, Department of Pharmacy
Microbial Pharmacology and Population Biology Research Group

Collateral sensitivity in clinical *Escherichia coli* isolates

Jessica Nguyen Tran

Supervisor: Professor Pål J. Johnsen, Ph.D.

Assistant supervisor: Nicole L. Podnecky, Ph.D.

Thesis for the degree Master of Pharmacy, May 2018



Acknowledgements

Firstly, I would like to thank the staff and faculty at the Microbial Pharmacology and Population Biology group at the department of Pharmacy, University of Tromsø – the Arctic University of Norway. Thank you for all your help and guidance in the laboratory during the past ten months. It has been a privilege working with you and being a part of your research group.

I would especially like to express my sincerest gratitude to my supervisors professor Pål J. Johnsen and postdoctoral fellow Nicole L. Podnecky. Thank you for taking the time to introduce me to the field of microbiology, for your patience, encouragement, enthusiasm and for sharing your knowledge and expertise. I am grateful for everything you have taught me throughout the process of researching and writing this thesis.

To my lovely Pharma-girls, thank you for five years' worth of continuous fun and excitement and the much-needed support. Thank you for listening and for all the advice. I would also like to thank my fellow students of the bachelor class of 2016 and the master class of 2018, this journey would never have been the same without all of you.

Finally, I would like to thank my beloved parents, siblings and boyfriend. I am forever grateful for your continuous support and unconditional love. Thank you for believing in me even when I didn't believe in myself. Cảm ơn anh, chị, ba và má vì đã luôn ủng hộ em út/con út.

Jessica Nguyen Tran

Tromsø, May 2018

Abstract

Background

At present time, antimicrobial resistance is emerging more rapidly than the development of novel antimicrobials, presenting a serious threat to how we prevent and treat infectious diseases. Several treatment strategies to counteract this development have been proposed, among these is the use of collateral sensitivity in clinical treatment. The ability to predict collateral sensitivity and cross-resistance effects is essential to exploiting this concept. In this study, we aimed to investigate the patterns of collateral sensitivity and cross-resistance in ciprofloxacin resistant isolates carrying *gyrA* and *parC* mutations.

Method

Ciprofloxacin resistant isolates were evolved from three clinical *E. coli* strain using static and dynamic selection methods. Isolates were selected based on identified mutations and level of ciprofloxacin resistance measured with diffusion gradient strips. DNA sequencing was used to detect mutations in *gyrA* and *parC*. Resistant isolates carrying at least one *gyrA* and *parC* mutation were characterized by IC₉₀ assays with micro-broth dilutions of six unrelated antimicrobial agents. The observed collateral sensitivity and cross-resistance effects were displayed in a heat map.

Results

Various non-synonymous point mutations in *gyrA* and *parC* were identified in several of the generated ciprofloxacin resistant isolates. These mutants displayed collateral sensitivity and cross-resistance to several unrelated antimicrobials. Collateral sensitivity to gentamicin and trimethoprim was observed in the majority isolates. Cross-resistance effects were found in several mutants, specifically to ceftazidime, chloramphenicol and colistin.

Conclusion

Our findings suggest that ciprofloxacin resistant mutants with *gyrA* and *parC* mutations display a clear tendency of collateral sensitivity to gentamicin, an effect which potentially can be exploited in future treatment. However, we propose further investigation into specific point mutations within these genes, to better understand the observed variations in collateral sensitivity and cross-resistance.

Table of contents

ACKNOWLEDGEMENTS	I
ABSTRACT.....	II
LIST OF FIGURES AND TABLES.....	IV
LIST OF ABBREVIATIONS	V
1 INTRODUCTION.....	1
1.2 PREFACE	1
1.3 MICROORGANISM OF INTEREST	2
1.4 ANTIMICROBIAL AGENTS.....	2
1.5 ANTIMICROBIAL RESISTANCE.....	6
1.6 MECHANISMS OF ANTIMICROBIAL RESISTANCE	7
1.7 STRATEGIES TO COMBAT ANTIMICROBIAL RESISTANCE	10
1.8 COLLATERAL SENSITIVITY	11
2 AIMS AND HYPOTHESIS.....	15
2.1 AIMS OF THIS STUDY.....	15
2.2 HYPOTHESIS.....	15
3 MATERIALS AND METHODS	17
3.1 BACTERIAL STRAINS.....	17
3.2 PREPARATION OF SOLID AND LIQUID GROWTH MEDIA AND OTHER SOLUTIONS	17
3.3 STANDARD TECHNIQUES FOR BACTERIAL CULTIVATION	18
3.4 STATIC SELECTION OF CIPROFLOXACIN RESISTANT MUTANTS	20
3.5 DYNAMIC SELECTION OF CIPROFLOXACIN RESISTANT MUTANTS	23
3.6 ISOLATION OF GENOMIC DNA.....	25
3.7 POLYMERASE CHAIN REACTION	26
3.8 AGAROSE GEL ELECTROPHORESIS.....	28
3.9 DNA SEQUENCING.....	29
3.10 ANTIMICROBIAL SUSCEPTIBILITY TESTING	30
4 EXPERIMENTAL RESULTS AND DISCUSSION.....	33
4.1 <i>E. COLI</i> ISOLATES CLINICALLY RESISTANT TO CIPROFLOXACIN	33
4.2 IDENTIFIED VARIATIONS IN RESISTANT ISOLATES.....	37
4.3 COLLATERAL SENSITIVITY AND CROSS-RESISTANCE PROFILES	42
4.4 CHALLENGES AND LIMITATIONS OF THIS STUDY	47
5 CONCLUSION AND FUTURE PROSPECTS.....	49
REFERENCES.....	51
APPENDICES.....	55

List of figures and tables

FIGURE 1.1: TIMELINE OF ANTIMICROBIAL DRUG DISCOVERY	1
FIGURE 1.2: HEAT MAP OF COLLATERAL CHANGES IN CIP ^R MUTANTS GENERATED BY PODNECKY ET AL	13
FIGURE 3.1: DEMONSTRATION OF 3-ZONE STREAK FOR ISOLATION	19
FIGURE 3.2: DEMONSTRATION OF SPREAD PLATING WITH GLASS BEADS.....	19
FIGURE 3.3: DEMONSTRATION OF SWAB PLATING ON ELECTRIC ROTATOR	19
FIGURE 3.4: A SCHEMATIC ILLUSTRATION OF THE DYNAMIC SELECTION METHOD	24
FIGURE 3.5: A SCHEMATIC ILLUSTRATION OF 1,5-FOLD DILUTION IN A 96-WELL PLATE.....	31
FIGURE 4.1: AN OVERVIEW OF SELECTION CONCENTRATION AND MUTANTS WITH CIP MIC \geq THE CLINICAL BREAKPOINT FOR FIRST STEP MUTANTS SORTED BY PARENTAL STRAIN	34
FIGURE 4.2: GEL IMAGE OF <i>GYRA</i> AMPLIFIED PCR PRODUCTS	37
FIGURE 4.3: GEL IMAGE OF <i>PARC</i> AMPLIFIED PCR PRODUCTS	38
FIGURE 4.4: HEAT MAP OF DRUG SUSCEPTIBILITY PROFILES OF CIP RESISTANT ISOLATES RELATIVE TO THEIR PARENTAL WT STRAIN.....	44
FIGURE 4.5: HEAT MAP COMPARING DRUG SUSCEPTIBILITY OF OUR CIP RESISTANT TO PREVIOUS WORK FROM PODNECKY <i>ET AL.</i> (CIP ^R).....	46
TABLE 3.1: <i>E. COLI</i> STRAINS USED IN THIS PROJECT	17
TABLE 3.2: CONCENTRATIONS OF CIP IN MHA SELECTIVE PLATES	21
TABLE 3.3: DILUTION SERIES FOR VIABLE CELL COUNT DETERMINATION	22
TABLE 3.4: SELECTION CONCENTRATION AND CIP VOLUME ADDED TO LIQUID MEDIA	23
TABLE 3.5: OVERVIEW OF PRIMERS USED FOR AMPLIFICATION OF <i>GYRA</i> AND <i>PARC</i> GENES.....	27
TABLE 3.6: COMPONENTS OF PCR SAMPLES	27
TABLE 3.7: SETTINGS FOR PCR WITH PHUSION HIGH-FIDELITY DNA POLYMERASE.....	28
TABLE 3.8: COMPONENTS OF THE DNA SEQUENCING SAMPLE	29
TABLE 3.9: OVERVIEW OF ANTIMICROBIAL AGENTS INCLUDED FOR IC90 TESTING	31
TABLE 4.1: OVERVIEW OF SECOND STEP MUTANTS GENERATED THROUGH DYNAMIC SELECTION AT SUB-MIC SELECTIVE CONCENTRATION	36
TABLE 4.2: OVERVIEW OF IDENTIFIED MUTATIONS IN CIP RESISTANT MUTANTS	39

List of abbreviations

A	Adenine (nucleobase), Alanine (amino acid)
Ad	Add to
AMR	Antimicrobial resistance
ATP	Adenosine triphosphate
C	Cytosine (nucleobase), Cysteine (amino acid)
CAZ	Ceftazidime
CFU	Colony forming units
CHL	Chloramphenicol
CIP	Ciprofloxacin
CIP ^R	Ciprofloxacin resistant mutant
CLSI	The Clinical and Laboratory Standards Institute
COL	Colistin
CR	Cross-resistance
CS	Collateral sensitivity
D	Aspartate
dH ₂ O	Distilled water
DNA	Deoxyribonucleic acid
dNTP	Deoxyribonucleotide triphosphate
E	Glutamate
<i>E. coli</i>	<i>Escherichia coli</i>
<i>e.g.</i>	For example
ECDC	European Centre for Disease Prevention and Control
EEA	The European economic area
EHEC	Enterohaemorrhagic <i>E. coli</i>
EMA	European medicines agency
EtBr	Ethidium bromide
ETEC	Enterotoxigenic <i>E. coli</i>
EtOH	Ethanol

EU	The European union
EUCAST	European Committee on Antimicrobial Susceptibility Testing
G	Guanine (nucleobase), glycine (amino acid)
GEN	Gentamicin
HGT	Horizontal gene transfer
HIV	Human immunodeficiency virus infection
I	Isoleucine
K	Lysine
L	Leucine
LB	Luria-Bertani broth
LBA	Luria-Bertani agar
LPS	Lipopolysaccharides
MHA	Mueller-Hinton agar
MHB	Mueller-Hinton broth
MIC	Minimal inhibitory concentration
MNEC	Meningitis-associated <i>E. coli</i>
mRNA	Messenger Ribonucleic acid
N	Asparagine
ng	Nanogram
PABA	Para-aminobenzoic acid
PCR	Polymerase chain reaction
PBP	Protein-binding proteins
QRDR	Quinolone-resistant determining region
R	Arginine
RNA	Ribonucleic acid
rpm	Rounds per minute
S	Serine
Sec	Seconds
SNP	Single nucleotide polymorphism
T	Thymidine

TAE	Tris-acetate-ethylenediaminetetraacetic acid
TMO	Temocillin
TMP	Trimethoprim
UNN	University Hospital of Northern Norway
UPEC	Uropathogenic <i>E. coli</i>
UTI	Urinary tract infections
WHO	World Health Organization
WT	Wild type

1 Introduction

1.1 Preface

The discovery of antibiotics during the 20th century made it possible to treat countless dangerous and deadly infectious diseases. Throughout the century, antibiotics significantly contributed to a reduction in morbidity and mortality and, among other factors, to an increase in life expectancy. Previously incurable infectious diseases with high prevalence and high mortality rates, such as tuberculosis and pneumonia, proved susceptible to the revolutionary drugs, resulting in higher survival rates, an increase in childbirth and an extended lifespan (1, 2).

In recent years the development of antimicrobial agents seems to have stagnated as it has proven to be increasingly difficult to discover new compounds. The accidental discovery of penicillin by Alexander Fleming in 1929 led to a major breakthrough in the treatment of infectious diseases, and initiated the golden age of antibiotic discovery (3). Following this discovery, was the introduction of the “Waksman platform” by Selman Waksman in the 1940s, which entailed screening soil streptomycetes for antimicrobial activity (4). This platform led to the discovery of multiple antibiotic classes in the following decades, as shown in **Figure 1.1**, that are still commonly used today. However, these victories eventually led to a diminished interest to continue developing new antimicrobial agents. The discovery of streptogramins in 1964 marked the end of an era, and the only antimicrobial discovery since was of the lipopeptide drug daptomycin in 1986 (4).

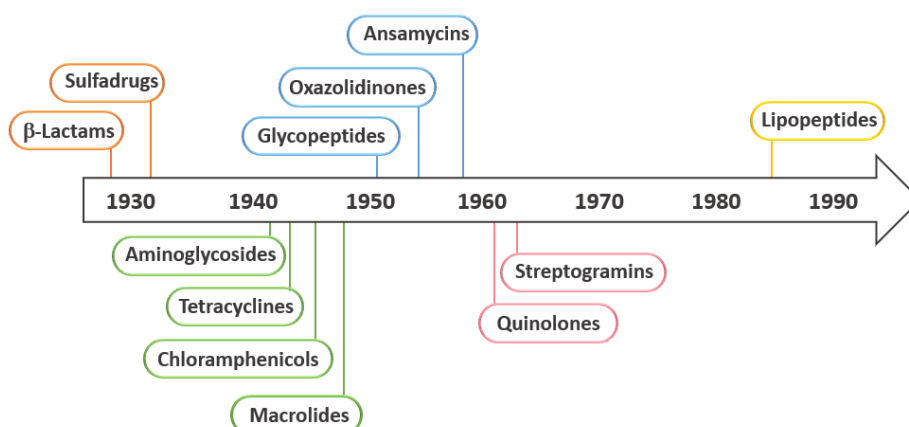


Figure 1.1: Timeline of antimicrobial drug discovery. Adapted from Lewis (4).

Increased access to antimicrobials over the following decades, combined with extensive and continuous misuse and overuse has inevitably led to the emergence of resistance. Antimicrobial resistance (AMR) presents a global threat that will greatly affect prevention and treatment of infectious diseases in the future (5). According to World Health Organization (WHO), known treatments are becoming less effective and an increasing number of infections are becoming more challenging to treat (6). Currently, antimicrobial resistance is emerging more rapidly than the development of novel antimicrobials, and there is an urgent need for more efficient ways to utilize current antimicrobials (2).

1.2 Microorganism of interest

Since its discovery in 1885, *Escherichia coli* has become a well-known and vastly studied bacterium (7). It is described as a rod-shaped, unpigmented, Gram-negative bacteria, commonly found in the human body as a part of the normal intestinal microflora (8). *E. coli* is a highly versatile microorganism with no growth factor requirements, meaning that it is able to grow with or without the presence of oxygen (9). Under healthy and uncompromised conditions in the host, *E. coli* serves a mutually beneficial role and rarely causes disease in humans and other mammals. However, as a result of acquiring specific virulence factors, some versatile pathogens of *E. coli* can gain the ability to colonize outside of their usual habitat thus potentially causing various diseases of different severity (10).

Pathogens of *E. coli* can mainly be divided into two categories, intestinal pathogenic *E. coli* and extraintestinal pathogenic *E. coli*, depending on their site of infection, respectively (8). The intestinal category includes pathotypes commonly causing diarrheal diseases such as enterohaemorrhagic *E. coli* (EHEC) which is highly associated with foodborne outbreaks and the travelers' diarrhea causing enterotoxigenic *E. coli* (ETEC), often found in contaminated water sources (8). Among the extraintestinal pathogens is the meningitis-associated *E. coli* (MNEC) responsible for sepsis and meningitis, as well as the pathotype uropathogenic *E. coli* (UPEC) which frequently causes urinary tract infections (8).

1.3 Antimicrobial agents

The term “antibiotics” was first mentioned and described by Selman Waksman in 1942 as “substances produced by microorganisms and which are antagonistic to the growth or life of

other microorganisms in high dilution” (3). This definition still applies today, but antibiotics are now more frequently referred to as antimicrobial agents, along with agents used against fungi, parasites and viruses (11). In addition to natural antimicrobials there are also numerous synthetic and semi-synthetic agents (11) on the market. Most agents extracted from microorganisms, *e.g.* penicillin, originally isolated from the fungus *Penicillium notatum* by Alexander Fleming in 1929 (3), have been chemically modified in order to enhance their pharmacological and antibacterial effects.

Antimicrobial agents can be classified as bactericidal or bacteriostatic agents, depending on whether they induce cell death or inhibit cell growth, respectively (12). However, they are more commonly divided into groups based on similarities in chemical structure and mode of action (11). Ideally an antimicrobial agent should target something that is present in bacterial cells and non-present in healthy mammalian cells. This selective toxicity is achieved through targeting the structural differences between eukaryotic and prokaryotic cells and there are five main target sites for which antimicrobials commonly disrupt the cellular functions of bacteria: cell wall synthesis, cell membrane function, protein synthesis, nucleic acid synthesis and metabolic pathways (11).

1.3.1 Cell wall synthesis

The cell wall in bacteria is a unique and complex multilayered structure that serves as a barrier to the outer environment as well as a protective layer for the interior. Peptidoglycan is an essential component of the cell wall in both Gram-negative and Gram-positive bacteria (13). Synthesis of peptidoglycan is a process that requires transport of peptide chains across the cytoplasmic membrane and their incorporation into the growing peptidoglycan backbone (11).

Several antimicrobial agents target the cell wall synthesis, such as the beta-lactams (*e.g.* penicillins, cephalosporins, monobactams) and glycopeptides (*e.g.* vancomycin, teicoplanin). Beta-lactams interact with penicillin-binding proteins (PBPs), enzymes that are responsible for the cross-linking of the peptide chains to the peptidoglycan. The formation of beta lactam-PBP complexes prevents cross-linking of the cell wall and lengthening of the peptidoglycan structure, inevitably leading to cell lysis. Glycopeptides inhibit cell wall synthesis at an earlier stage than beta lactams, they bind to the terminal end of pentapeptide chains, thereby preventing insertion into the growing peptidoglycan backbone (11, 14).

1.3.2 Cell membrane function

Lipopeptides (*e.g.* daptomycin) and polymyxins (*e.g.* polymyxin B, colistin) are groups of antimicrobial agents that inhibit the cell membrane function (11, 14). Polymyxins are bactericidal agents that act as cationic detergents (14), meaning that they bind to the bacterial lipopolysaccharides (LPS) and displace the divalent cations, leading to a disorganized bilayer structure which alters the permeability of the cell membrane (15). Lipopeptides are a relatively new class of antimicrobials, discovered in 1986 (as shown in **Figure 1.1**), and their mode of action has yet to be clearly understood. However, it has been suggested that daptomycin acts by binding to the bacterial cytoplasmic membrane, resulting in the loss of potassium from the bacterial cell which inhibits the synthesis of ATP and limits the uptake of necessary nutrients (11, 16).

1.3.3 Protein synthesis

Proteins are generated through a process that involves the transcription of RNA and the translation of mRNA. Bacterial ribosomes are essential for protein synthesis and serves as a decoding site for mRNA into amino acid chains through multiple steps. The bacterial ribosomes are composed of two subunits, a larger 50S subunit and a smaller 30S subunit (17). Differences in the composition of ribosomes in eukaryotic and prokaryotic cells allows for selective toxicity of antimicrobials (11).

The macrolides, aminoglycosides and tetracyclines are groups of antimicrobial agents that target protein synthesis in bacterial cells. Aminoglycosides (*e.g.* gentamicin and tobramycin) disrupt the protein synthesis by binding to the 30S subunit, where they interfere with the binding of formylmethionyl-transfer RNA (fmet-tRNA), which is essential for the initiation of the protein synthesis (11). Tetracyclines (*e.g.* tetracycline and doxycycline) bind the smaller ribosomal subunit, 30S, and prevent the access of amino-acryl transfer RNA carrying amino acids to the ribosome (18). Chloramphenicol blocks the formation of peptide bonds by binding the 50S subunit and inhibiting the catalyzing enzyme, peptidyl transferase. Macrolides (*e.g.* erythromycin and azithromycin) also act by irreversibly binding to the 50S subunit and inhibit the translocation step in protein synthesis (11, 14).

1.3.4 Nucleic acid synthesis

There are various ways by which antibacterial agents can inhibit nucleic acid synthesis in bacteria, for example by inhibiting RNA transcription (*e.g.* rifampicin) or directly inhibiting DNA replication (*e.g.* ciprofloxacin). Rifampicin binds with high affinity to the RNA polymerase enzymes, preventing the synthesis of mRNA (11, 18). This eventually halts the RNA transcription, as mRNA is the basis for protein translation and encodes for amino acid sequences. Ciprofloxacin and fluoroquinolones are of great relevance in this study and will be discussed more specifically in **Section 1.3.6**.

1.3.5 Metabolic pathways

Sulphonamides and trimethoprim are examples of antimicrobial agents that affects a metabolic pathway in bacterial cells. Their mode of action is by inhibiting the synthesis of tetrahydrofolic acid, a precursor molecule essential in the synthesis of necessary nucleic acids (11). The sulfonamides (*e.g.* sulfamethoxazole, sulfadiazine) are structural analogues of para-aminobenzoic acid (PABA) (14). They competitively bind and inhibit dihydropteroate synthetase, an enzyme which normally catalyzes a reaction in the synthesis of tetrahydrofolic acid. A reduced ability to synthesize tetrahydrofolic acid, further prevents the synthesis of DNA and RNA (14). In a similar manner, trimethoprim also prevents the synthesis of tetrahydrofolate by binding to the dihydrofolate reductase enzyme and inhibiting at a later stage in the pathway (11).

1.3.6 Ciprofloxacin

Ciprofloxacin (CIP) is a bactericidal drug in the fluoroquinolone group of antimicrobials. It acts by binding and inhibiting the topoisomerase enzymes II (DNA gyrase) and IV, which are necessary enzymes for replication of the bacterial chromosome (11). DNA gyrase consists of two subunits, GyrA and GyrB, encoded by the *gyrA* and *gyrB* genes (19). Prior to replication, DNA gyrase is responsible for introducing a negative superhelical twist to the double-stranded bacterial DNA. This is a crucial step for the initiation of DNA replication. Similarly to DNA gyrase, topoisomerase IV is composed of the two subunits, ParC and ParE encoded by the *parC* and *parE* genes. After a round of replication, topoisomerase IV removes the interlinking between two daughter chromosomes, ensuring proper segregation (19).

The ability of CIP to kill bacteria is dependent on the stability of the ternary complex formed upon binding of the drug to the topoisomerase-DNA complexes (18, 20). Enzyme-DNA complexes are formed during normal replication (20). Binding of the drug to these complexes occurs prior to DNA-cleavage and affects the ability to cleave DNA which leads to DNA strand breakage (18). As a result of this interaction, DNA replication is inhibited, which halts the DNA synthesis and eventually leads to cell death (18-20).

CIP can be used in the treatment of respiratory, ear, gastrointestinal, genital and urinary tract infections (21). However, in the Norwegian guidelines (22), CIP is rarely regarded as a treatment option, and it is advised to use it restrictively. Restrictions in treatment are likely due to the fact that CIP is a broad-spectrum antimicrobial and it is believed that replacement of broad-spectrum with narrow-spectrum antimicrobials during treatment may contribute to reduced evolution and spread of resistance (23). For the treatment of cystitis, the guidelines state that fluoroquinolones should only be considered in complicated cases of cystitis and when resistance to the conventional treatment options is present. Conventional treatment options include nitrofurantoin, pivmecillinam and trimethoprim, none is regarded as the superior alternative (22).

1.4 Antimicrobial resistance

Antimicrobial resistance can be defined in multiple ways. From a medical perspective, a resistant organism is defined as “an organism that will not be inhibited or killed by an antimicrobial agent at concentrations of the drug achievable in the body after normal dosage” (11). Antimicrobial resistance is often a result of the selection of microorganisms during exposure to a hostile antimicrobial environment. The inappropriate use of antimicrobials through decades has prompted microorganisms to develop sophisticated survival mechanisms (24). The specifics of these mechanisms will be discussed further in **Section 1.5**.

Increased prevalence of antimicrobial resistance puts great pressure on the public health systems, mostly due to a rise in the number health-care associated infections, hospital admissions and a reduced capacity of health personnel and medical care (25, 26). Resistance can also present serious health risks to the population, as it makes finding the correct treatment more challenging resulting in longer illness duration and higher mortality rates (26). Studies have shown that discrepancies between the given treatment and susceptibility test results are a

main factor in delayed administration of effective therapy, which eventually may lead to unfavorable outcomes (27). Effective courses of treatment are often more comprehensive and can be associated with toxic and adverse effects (27).

In addition to the health risks and therapeutic consequences, antimicrobial resistance also has a major impact on the economy. A joint technical report from the European Centre for Disease Prevention and Control (ECDC) and The European Medicines Agency (EMA) from 2009, predicted additional costs in healthcare and productivity losses, due to patient fatalities, to about 1,5 billion euros annually for every nation in the EU/EEA (28).

1.5 Mechanisms of antimicrobial resistance

Resistance mechanisms in microorganisms can be divided into three main categories; intrinsic, acquired or adapted. Intrinsic resistance is due to naturally-occurring properties possessed and inherited by the microorganism that restricts the action of certain antimicrobial compounds (29). Intrinsic resistance to one or multiple antimicrobial agents is commonly due to drug impermeability or enzymatic inactivation of the drug, multidrug efflux pump activity and/or lack of susceptible drug targets (11). Intrinsic clearance can be found in Gram negative bacteria, which are naturally resistant to glycopeptides due to the size of the drug making it unable to efficiently penetrate the outer membrane (11). However, a larger threat is when resistance is observed in a population that was originally susceptible to an antimicrobial drug. Antimicrobial resistance under these circumstances is referred to as acquired resistance. Acquired resistance is often the result of chromosomal mutations associated with potential drug targets or external transmission of resistant genes through horizontal gene transfer (24). Both mechanisms will be discussed further in the sections below. Adapted resistance further differs from both intrinsic and acquired as it is an unstable and reversible state of increased ability to survive exposure to antimicrobials. Adapted resistance is usually caused by temporary alterations to gene and/or protein expression triggered by various environmental factors, *e.g.* nutrient conditions or the antimicrobial compound itself (29).

1.5.1 Horizontal gene transfer (HGT)

The spread of resistance traits can occur vertically by replication, where resistant genes are inherited through generations of bacterial reproduction. Alternatively, resistant genes can be exchanged horizontally between unrelated bacteria, which occurs more frequently between

highly similar species. Acquisition of external genetic material between bacteria can be divided into three main mechanisms, formally known as transformation, transduction and conjugation (30).

Transformation describes a process where foreign DNA from the surrounding environment is taken up, incorporated and functionally expressed under normal growth circumstances in a bacterial recipient cell. To undergo such a process the recipient cell must be competent, meaning it has to enter a certain physiological state regulated by growth environment and other factors (31). During conjugation genetic material is transferred from a donor to a recipient cell through physical contact, this stable physical cell-to-cell contact is mediated by a conjugation pilus of the donor cell (30). Direct transfer of genetic material between chromosomes can occur under conjugation, but the use of mobile genetic elements (such as plasmids and transposons) as vehicles are more common (24). Transduction is used to describe the movement of genetic material from one bacteria to another through DNA-carrying viruses, the bacteriophages. Packed DNA in fully-functional bacteriophages are delivered from an infected bacterium to a suitable and susceptible bacterium and further incorporated into their genome (31).

1.5.2 Mutations in chromosomal genes

Gene mutations describe the change of nucleotides within the DNA sequence of a gene. These mutations can be induced through exposure to mutagens, environmental agents that increase the rate of mutation occurrence, or they may arise spontaneously without external treatment by naturally-occurring damages during DNA replication. Point mutations are alterations that affect a single site within a gene, either one single base of DNA or a small number of neighboring base pairs. Point mutations can be the result of base substitutions, additions or deletions. A single base pair substitution, also known as single nucleotide polymorphism (SNP), involves the replacement of a base pair by another, which can occur by transition (replacement base from within the same chemical category, *e.g.* pyrimidine replaced by pyrimidine) or transversion (replacement base from another chemical category, *e.g.* purine replaced by pyrimidine). DNA insertions or deletions, simply termed indel mutations, involves the addition or removal of a single or multiple base pair(s) (32).

Potential molecular consequences of point mutations may vary in terms of severity, in some cases the effect can be beneficial and the bacteria gains new functions, in other cases the

mutation contributes to a loss of function, which may be harmful to the cell. Indel mutations can shift the reading frame of protein-coding DNA and potentially alter the protein structure and function. Base substitutions can potentially cause synonymous or non-synonymous mutations. Synonymous mutations, also known as silent mutations, are caused by base pair substitutions that alter the amino acid codon, but maintain the same amino acid. Thus, a silent mutation does not alter the amino acid sequence or protein expression. The opposite of a silent mutation, is a non-synonymous mutation caused by nucleotide substitutions that alter the amino acid codon and sequence, which further changes the protein structure. Nonsense mutations is a form of non-synonymous mutations, where an amino acid codon is changed into a translation termination codon that causes protein translation to terminate prematurely (32).

1.5.3 Fluoroquinolone resistance in *E. coli*

Resistance to fluoroquinolones can be acquired through modification of drug target enzymes or reducing drug accumulation within the cell. Plasmid-mediated resistance has also been reported in *E. coli* (19, 33). Resistance due to modified target enzymes are often caused by direct mutations to the genes, which alter the binding site and reduce drug affinity. Alterations in *gyrA* occur more frequently than in *gyrB*, and likewise more frequently in *parC* than in *parE* (19). In resistant *E. coli* isolates, *gyrA* mutations are often found between the 67 and 106 amino acids, this is also known as the quinolone-resistant determining region (QRDR). Equivalently, mutations contributing to resistance have been found in the QRDR of the *parC* subunit. Generally, *gyrA* mutations occurs prior to *parC* mutations in *E. coli* as DNA gyrase in Gram-negative bacteria is intrinsically more susceptible to quinolones (19, 33).

Reduced access to the drug targets in Gram-negative bacteria can be the result of the altered expression of membrane porins or efflux-pump systems. To interact with the enzyme targets quinolones have to traverse the cell wall as well as the cytoplasm membrane. Entrance of quinolones to the cytoplasm in Gram-negative bacteria occurs by passive diffusion through outer membrane porins (33). Reduced expression of membrane proteins, such as OmpF and OmpC in *E. coli*, alters the permeability and contributes to a reduced influx of drugs. Additionally, bacteria have efflux-pump systems, which are membrane-associated, energy-dependent systems that are able to extrude quinolones, along with other antimicrobial agents and harmful substances, from the cell interior. Mutations to certain genes encoding for transcriptional regulators can result in the overexpression of such systems, which consequently

decreases the amount of drug accumulating within the cell and thus the ability of the drug to reach the target. In *E. coli*, mutations to *acrR* and *marR*, encoding regulators of the AcrAB-TolC efflux pump, have been shown to have a large impact on the efflux of quinolones, as well as several other antimicrobial agents, such as tetracycline, chloramphenicol and erythromycin (34). Thus, efflux pump systems can greatly contribute to multidrug resistance.

Resistance to quinolones in *E. coli* can also be acquired through plasmids. Plasmid-mediated resistance to quinolones can mainly be caused by three genes, *qnr*, *Aac(6′)-Ib-cr* or *qepA* (35). The Qnr protein, encoded by the *qnr* gene, interferes with the binding of quinolones to the topoisomerase-DNA complexes likely by altering the binding properties of the complex (35). The *Aac(6′)-Ib-cr* gene encodes for the quinolone-acetylating Aac(6′)-Ib-cr enzyme, which inactivates certain quinolones, such as ciprofloxacin and norfloxacin, by introducing an additional acetyl substituent. However, the activity of the Aac(6′)-Ib-cr enzyme is limited to quinolones with a unsubstituted piperazinyl nitrogen group. The *qepA* gene encodes for an efflux pump that is able to extrude quinolones, such as ciprofloxacin and norfloxacin (35).

1.6 Strategies to combat antimicrobial resistance

Conventional antimicrobials are becoming insufficient for the treatment of drug-resistant infections and the development of novel antimicrobials appears to have stagnated. In order to avoid the possibility of a post-antibiotic era, several methods have been proposed in order to prevent and minimize the emergence of resistance as well as extend the use of existing antimicrobial agents. Among others, these include more rational use of antimicrobials, meaning a reduction in unnecessary treatment with antimicrobials, more accurate prescriptions, restrictions in the use of broad-spectrum antimicrobials and more controlled therapeutic use in animals and in agriculture (2, 23). The O’Neill review on tackling AMR from 2016 also suggests implementing measures to increase public awareness, improve hygiene, and prevent the spread as well as to promote alternatives such as vaccines (36).

Combination therapy is also a promising strategy that has been exploited and established in the treatment of several infectious diseases, such tuberculosis and HIV (37). Generally, antimicrobial agents can be combined in three ways; inhibit the same target through different pathways, inhibit different targets through the same pathways or inhibit the same target in distinct ways. Treatment with two or several antimicrobials can potentially reduce the dosage

necessary of each drug, the risk of resistance development and the risk of adverse effects. However, a challenge associated with combining multiple antimicrobial agents are the unpredictable toxicity, as well as changes to the pharmacokinetic and pharmacodynamic profiles (37).

Recently, infection treatments informed by principles of evolutionary biology have received significant attention. These alternative strategies are collectively termed “selection inversion” and include the use of drug suppressive interactions, synergy-inducing drug pairs and collateral sensitivity (38). Drug suppressive interactions requires co-administration of two antimicrobials and are based on using drug concentrations that inhibits resistance by selecting against single-drug resistant mutants, as the drug-sensitive parental strain will outcompete resistant mutants. The use of synergy-inducing drug pairs is a hypothetical strategy that involves using drug combinations that acts more synergistic in resistant mutants in comparison to the sensitive parental strain (38). Collateral sensitivity is a particularly promising strategy that selects against resistance without the need for co-administration, this will be discussed further in **Section 1.7**.

1.7 Collateral sensitivity

As pioneers of their time, Szybalski and Bryson encountered the phenomenon they named collateral sensitivity (CS) in 1952 during their experiments to investigate changes to the susceptibility profile of antimicrobial-resistant *E. coli* (39). The term collateral sensitivity was used to describe the occurrence of increased sensitivity to other unrelated antimicrobial agents, while a decrease in sensitivity was regarded as cross-resistance (CR). Although the underlying mechanisms of collateral sensitivity remain largely unknown, it more recently was recognized as a unique and promising novel strategy to combat the emergence of resistance. The concept of CS is simply understood by the evolutionary principle of trade-offs; meaning losing one quality or aspect in return for another, which in this case translates to losing sensitivity to an antimicrobial agent(s) in return for increased sensitivity towards another agent(s) (40).

In 2013, Imamovic and Sommer proposed the use of collateral networks to inform drug cycling as an approach for more sustainable use of antimicrobials (41). Their distinct and innovative approach to drug cycling is based on exploiting the reciprocal hyper-sensitivity to unrelated agents found in AMR organisms. As resistance to an antimicrobial agent emerges during treatment, eventually leading to ineffective treatment, the organism becomes more susceptible

to another unrelated agent. Switching treatment to the latter alternative, to which the resistant isolate is now more sensitive, would either kill the organism or force it to survive by developing resistance to the second drug, ideally gaining hyper-sensitivity back to the initial agent. Re-initiating treatment with the starting agent could prove beneficial as the organism would be more susceptible than it initially was. Rotating in this scheduled manner may improve and enable effective treatment with current antimicrobials (41).

The ability to predict CS effects, and in turn select effective antimicrobial agents in clinical treatment, is essential prior to exploiting CS networks in drug cycling and combination therapy. However, this greatly relies on extending our knowledge of the susceptibility patterns of drug resistant organisms. Several studies have investigated the changes in susceptibility to numerous antimicrobial agents (40-42), however, our knowledge is limited in terms of understanding the underlying mechanisms of CS and variation in CS effect caused by specific resistance mechanisms.

However, in a previous study by Lazar *et al.* it was suggested that observed CS patterns in aminoglycoside-resistant organisms can be linked to the reduced function of the AcrAB efflux system due to mutations (43). They were able to confirm this by testing aminoglycoside resistant mutants against several antimicrobial agents that were known substrates of the AcrAB efflux system, and observed CS to all agents tested against mutants with impaired efflux systems. They also found that the damaged function of the AcrAB efflux system leading to the CS effects observed, is a result of mutations contributing to reduced membrane potential (43).

The basis of this particular study is the previous work by Podnecky *et al.* mapping the susceptibility patterns of CIP resistant (CIP^R) *E. coli* isolates to several unrelated antimicrobial agents (42). Observed collateral effects of ten CIP^R mutants generated from ten various strains were assembled in a heat map, **Figure 1.2**. The majority of CIP^R mutants (nine of ten) displayed CS to gentamicin. Of these the K56-2 CIP^R mutant was the only isolate carrying both *gyrA* and *parC* mutations, which is the most frequently found mutation in clinical CIP resistant isolates (42, 44, 45). The K56-2 CIP^R mutant also displayed CS to azitromycin and ertapenem, as shown in **Figure 1.2**. Generally, CR was observed less in the K56-2 CIP^R mutant, compared to the other strains, that all carried efflux pump mutations (42).

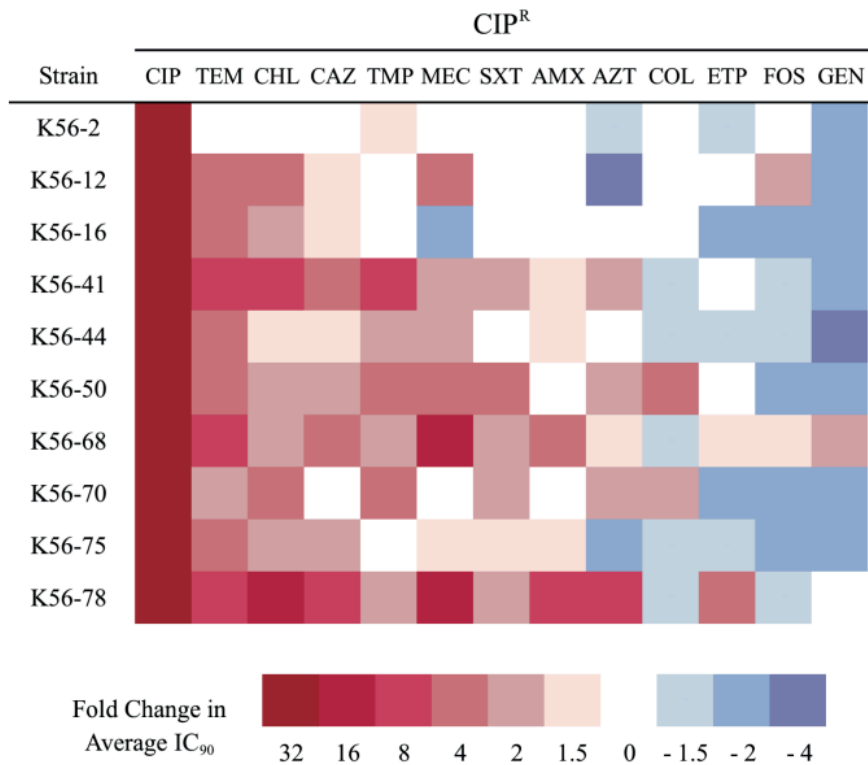


Figure 1.2: Heat map of collateral changes in CIP^R mutants generated by Podnecky *et al.* Increased susceptibility is shown in blue and decreased susceptibility is shown in red. Abbreviations of antimicrobial agents: amoxicillin (AMX), azithromycin (AZT), ceftazidime (CAZ), chloramphenicol (CHL), ciprofloxacin (CIP), colistin (COL), sulphamethoxazole/trimethoprim (SXT), ertapenem (ETP), fosfomycin (FOS), gentamicin (GEN), mecillinam (MEC), trimethoprim (TMP), temocillin (TEM). Figure adapted from Podnecky *et al.* (42).

2 Aims and hypothesis

2.1 Aims of this study

In clinical *E. coli* isolates a common cause for CIP resistance is mutations in the drug targets, DNA gyrase and topoisomerase IV, *gyrA* and *parC* genes respectively. Although such mutations are more prevalent, mutations in the efflux regulator genes can also contribute to resistance (44, 45). Preliminary data from the previous studies by the Microbial Pharmacology and Population Biology (MicroPop) research group (42) suggest a possible CS effect to gentamicin in CIP^R isolates carrying either a combination of *gyrA* and efflux-pump mutations or *gyrA* and *parC* mutations. However, CS to gentamicin was only observed in one resistant isolate with *gyrA* and *parC* mutations.

The aim of this study is to investigate whether these findings are general, caused by resistance development to CIP, or if they are related to specific mutations; meaning that different genetic alterations would cause variation in CR and CS.

2.2 Hypothesis

We hypothesize that collateral sensitivity to gentamicin in CIP resistant *E. coli* isolates, with mutations in *gyrA* and *parC*, is a general feature of homologous *E. coli* strains and not related to strain background. It is also believed that different strains with the same point mutations will exhibit the same patterns of CS and CR.

3 Materials and methods

3.1 Bacterial strains

The bacterial strains used to generate CIP resistant mutants in this project, listed in **Table 3.1**, were isolated from cases of acute, non-recurrent, uncomplicated urinary tract infections as part of the multinational and multicenter ECO-SENS study (46). The control strain ATCC 25922, was also included for antimicrobial susceptibility testing.

Table 3.1: *E. coli* strains used in this project

Strain	Sequence type	Phylogroup	Year	Country of origin
K56-2	ST73	B2	2000	Greece
K56-12	ST104	B2	2000	Portugal
K56-78	ST1235	D	2007-2008	United Kingdom

3.2 Preparation of solid and liquid growth media and other solutions

3.2.1 Luria-Bertani medium

Luria-Bertani medium is commonly used for the cultivation of *E. coli* in laboratory settings. It provides a broad base of nutrients and is suitable for both liquid and solid bacteria cultivation.

Liquid LB media (LB) was prepared by adding 12 g of Luria-Bertani broth (Sigma-Aldrich, USA) to 800 mL of distilled water (dH₂O) in a Pyrex glass bottle and autoclaved at 121°C for 20 minutes. The media was then cooled to room temperature and stored at 4°C. LB agar (LBA) plates were prepared by combining 12 g of Luria-Bertani broth, 10 g of Select agar (Sigma-Aldrich, USA) and 800 mL of distilled water (dH₂O) in a Pyrex glass bottle and autoclaved at 121°C for 20 minutes. After autoclaving, the medium was cooled to approximately 50°C on a magnetic stirrer and poured onto sterile petri dishes. The plates were left to solidify at room temperature overnight and stored at 4°C.

3.2.2 Muller-Hinton II medium

Cation-adjusted Mueller Hinton (MH) is a non-selective and non-differential media, and the preferred standard media for susceptibility testing, that complies with the EUCAST (European

Committee on Antimicrobial Susceptibility Testing) and CLSI (Clinical and Laboratory Standards Institute) guidelines for antimicrobial susceptibility testing. In this project, MH broth (MHB) and MH agar (MHA) were mainly used for susceptibility testing and static selection of mutants.

MH broth (BD, USA) and MH agar (BD, USA) plates for susceptibility testing were obtained from the University of Northern Norway (UNN) in Tromsø. Regular MH agar (Sigma-Aldrich, USA) for selection was prepared in the laboratory as specified by the manufacturer. Usually 800 mL of distilled water (dH₂O) was added to 30,4 g of MHA in a glass bottle and autoclaved at 121°C for 20 minutes, before it was cooled to approximately 50°C on a magnetic stirrer. The liquid media was then poured onto petri-plates and solidified at room temperature overnight and eventually stored at 4°C.

3.2.3 Ciprofloxacin stock solution

A stock solution of 25 mg/mL was prepared by dissolving 96,17 mg of ciprofloxacin (Sigma-Aldrich, USA) into 3,7739 mL of 0,1 M HCl. The solution was then sterilized using a 0,2 µM filter (Pall Acrodisc, USA), aliquoted into smaller volumes of 200 µl and stored at -20°C.

3.3 Standard techniques for bacterial cultivation

Bacteria were cultivated in either appropriate liquid or solid media, depending on its downstream use. The techniques used are described in the sections below.

3.3.1 Techniques for plating on solid media

3.3.1.1 Streak for isolation

To streak for isolation, a sterile loop was used to transfer the inoculum to the agar plate. Then, using the same loop, zone 1 was struck by moving the loop back and forth to create a zigzag pattern, covering one-third of the plate. A new sterile loop was then used to drag a few lines from zone 1 to create zone 2 continuing in the zigzag motion, as illustrated in **Figure 3.1**. The same loop was then turned over and the opposite side was used to streak a few lines from zone 2 to zone 3, covering the remaining space on the plate without touching any of the previous zones.

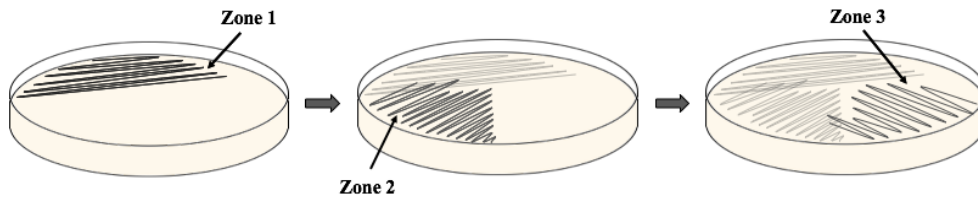


Figure 3.1: Demonstration of 3-zone streak for isolation

When using the 3-zone streak for isolation technique, the inoculum was gradually diluted from a high concentration of bacteria that showed heavy growth, to a lower concentration with less growth and more single isolated colonies, making it an ideal method for when separation of pure isolated colonies was necessary.

3.3.1.2 Spread plating with glass beads

Spread plating with glass beads was a method used to ensure even distribution of a liquid inoculum on an agar plate. Approximately 15-20 sterile glass beads were poured on to a plate, followed by adding a volume of the desired liquid culture. The plate was then shaken horizontally until the inoculum was fully absorbed, as illustrated in **Figure 3.2**, before removal of the glass beads.

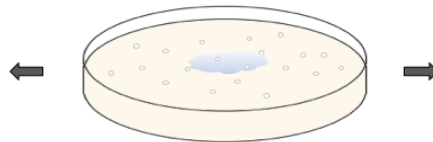


Figure 3.2: Demonstration of spread plating with glass beads

3.3.1.3 Swab plating

Swab plating on an electrical rotator was used to achieve uniform plating. This technique was mostly used for antimicrobial susceptibility testing with gradient diffusion strips.

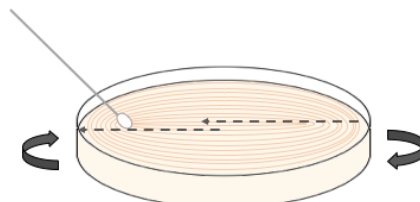


Figure 3.3: Demonstration of swab plating on electric rotator

The plate was placed on the rotator and a sterile cotton swab dipped in a 0,5 McFarland suspension was used to slowly draw a line from the edge towards the center of the plate applying gentle pressure. Using the opposite side of the cotton swab, a new line was drawn starting from the center of the plate and moving towards the edge, as illustrated in **Figure 3.3**.

3.3.2 Overnight cultures in liquid media

Overnight cultures were prepared in either LB or MHB. A small amount of the bacteria or colony of interest was collected with a sterile loop directly from a freeze-stock culture or from growth on agar plates and re-suspended in the selected liquid media. The cultures were then incubated overnight at 37°C with shaking at 150 rpm. The volume of liquid media varied depending on the downstream use of the overnight sample. Generally, 5 mL of broth prepared in a sterile tube with venting was used to make the overnight samples intended for freeze-stock cultures or DNA isolation. For the selection of CIP mutants, between 25-60 mL of liquid media was used to make the overnight samples, these were prepared in sterile 100 mL flasks.

3.3.3 Glycerol freeze-stock cultures

Glycerol freeze-stock cultures allows for long-term storage of bacterial cultures, and were prepared for specifically-selected CIP resistant mutants after every successful selection step. A volume of the overnight culture of a strain or mutant of interest (see **Section 3.3.2**) was added to glycerol 80% in a sterile cryovial to yield a concentration of approximately 20% glycerol. Generally, 1500 µl of the overnight culture was combined with 500 µl of 80 % glycerol. The glycerol freeze-stocks were stored at -80°C.

3.4 Static selection of ciprofloxacin resistant mutants

The static selection method was initially used for generating CIP resistant mutants. Using this method mutants were evolved through multiple selection steps on solid growth media, with a gradual increase in selection concentrations.

3.4.1 Preparation of ciprofloxacin selective plates

MHA was prepared as specified by the manufacturer (see **Section 3.2.2**). Prior to pouring the media onto sterile petri-plates, a specific amount of CIP stock solution was added to the mixture to give the desired final drug-concentration (see **Table 3.2**). The plates were then left to be

solidified in room temperature overnight and stored at 4°C for a maximum of 2 weeks, due to the risks of evaporation and potential breakdown of the added drug.

Table 3.2: Concentrations of CIP in MHA selective plates

MHA II CIP plate	Volume of CIP stock solution (25 µl/mL) added to 800 mL of MH agar (µl)	Final concentration of CIP (µg/mL)
CIP _{0,016}	0,256	0,016
CIP _{0,032}	0,512	0,032
CIP _{0,064}	1,024	0.064
CIP _{0,128}	2,048	0,128
CIP _{0,25}	4	0,25
CIP _{0,5}	8	0,5
CIP ₁	16	1
CIP ₄	64	4
CIP ₈	128	8

3.4.2 Generating ciprofloxacin resistant mutants on solid media

The selection inoculum was prepared by making an overnight culture of the isolate of interest directly taken from a freeze-stock culture and suspended in MH broth (see **Section 3.3.2**). The following day, 10-20 mL of the inoculum was centrifuged at 4000 rpm for 10-20 minutes. The supernatant was discarded and the pellets were re-suspended thoroughly in 0,5-1 mL of MH broth. Afterwards, on selective MHA plates with the desired CIP concentration (listed in **Table 3.2**), 100 µl of the inoculum was plated on each concentration using the spread plating technique (see **Section 3.3.1.2**). An additional 100 µl of the suspension was collected for quantification of the initial inoculum and determination of mutation frequency (see **Section 3.4.3**). The plates were incubated for 24-48 hours, dependent on the observed growth.

For plates with observed growth, single isolated colonies were chosen for further study. Generally, the single colonies biggest in size and most similar to the wild type were chosen and at least 5 mutants for each strain was chosen after every selection step. These were re-streaked for isolation on new selective plates with the same concentration of CIP as their initial selection concentration. The plates were then incubated overnight at 37°C. The following day, overnight cultures were prepared in MH broth (see **Section 3.3.2**) by selecting a single isolated colony

from each plate and inoculating them separately. Freeze-stock cultures were then prepared and stored at -80°C.

3.4.3 Determination of initial inoculum and mutation frequency

To determine the mutation frequency, a serial dilution of the initial inoculum was setup. In a sterile 96-well plate, 9 wells per sample was filled with 225 µl of 0,85% saline. Then 25 µl of the inoculum was pipetted in to the first well of the dilution series and mixed thoroughly. In the following steps, 25 µl from the previous well was transferred to the next, as shown in **Table 3.3**, until the whole dilution series was completed. Pipet tips were discarded between each step. Afterwards, 100 µl of appropriate dilutions were plated on non-selective MHA plates using the spread plating technique (see **Section 3.3.1.2**) and incubated overnight at 37°C. The following day, the number of colonies were counted for each dilution plate.

Table 3.3: Dilution series for viable cell count determination

Dilution step	1	2	3	4	5	6	7	8	9
Dilution	1:10	1:10	1:10	1:10	1:10	1:10	1:10	1:10	1:10
Inoculum (µl)	25	25	25	25	25	25	25	25	25
Diluent volume (µl)	225	225	225	225	225	225	225	225	225
Total dilution factor	10 ⁻¹	10 ⁻²	10 ⁻³	10 ⁻⁴	10 ⁻⁵	10 ⁻⁶	10 ⁻⁷	10 ⁻⁸	10 ⁻⁹
Expected plate count (CFU/100 µl)	10 ⁹	10 ⁸	10 ⁷	10 ⁶	10 ⁵	10 ⁴	10 ³	100	10

The mutation frequency was calculated by first determining the total number of bacteria (colony forming units, CFU) plated. Total bacteria plated was calculated by multiplying the number of counted colonies with the dilution factor (dilution factors are shown in **Table 3.3**), as expressed in the following equation:

$$\text{Total bacteria plated (CFU)} = \text{dilution factor} \times \text{counted colonies dilution plate} \left(\frac{\text{CFU}}{100 \mu\text{l}} \right)$$

Mutation frequency expresses the ratio of plated bacteria able to grow in the presence of a certain CIP concentration. The frequency was calculated by dividing the number of mutants, or colonies observed on the selective plate, by the calculated number of total bacteria plated, as shown in the following equation:

$$\text{Mutation frequency} = \frac{\text{colony count on selective plate}}{\text{Total bacteria plated (CFU)}}$$

3.5 Dynamic selection of ciprofloxacin resistant mutants

The second method used for selecting spontaneously evolved CIP resistant isolates was through passaging. This was based on a method where the authors, through a similar approach, had successfully selected for *parC* mutations (45). Mutants were selected under a lower constant antimicrobial pressure compared to the static selection method, where the antimicrobial pressure was gradually increased over time.

3.5.1 Preparation of the selection inoculum

Streaks for isolation of the ten first step mutants generated through the static selection method were prepared from the glycerol freeze-stock cultures on separate non-selective MHA plates and incubated overnight at 37°C. After 16-18 hours, the selection inoculum was prepared by combining single colonies (one colony of each of the mutant from the same parental strain), as illustrated in **Figure 3.4**. The single colonies were picked using a loop and suspended in 25 mL of LB broth, then incubated overnight at 37°C with shaking at 150 rpm.

3.5.2 Preparation of ciprofloxacin selective liquid media

To prepare the selective liquid media, a specific amount of CIP was added to LB broth to a concentration equivalent to 0,5× the MIC for each strain. The MIC values were measured with diffusion gradient strips (see **Section 3.10.1**) and averaged for all the 1st step mutants (listed in **Appendix A**), and the selection concentration was calculated accordingly. **Table 3.4** shows an overview of the concentrations of CIP in the selective media and the corresponding amount of CIP stock solution added.

Table 3.4: Selection concentration and CIP volume added to liquid media

Strain	Volume of CIP stock solution (0,05 mg/mL) added to 50 mL of LB broth (µl)	Final concentration of CIP (µg/mL)
K56-2	176	0,176
K56-12	194	0,194
K56-78	158	0,158

3.5.3 Generating ciprofloxacin mutant by passaging in liquid media

The first passaging was performed by transferring 5 mL of the selection inoculum to 45 mL of LB broth containing a specific amount of CIP added prior to the transfer. Transfers were performed in two parallels of 50 mL in 100 mL flask for each of the strains. The flasks were then incubated at 37°C with shaking at 150 rpm for 12 hours.

The following transfers were executed every 12 hours \pm 30 min, in a similar manner; 5 mL of the previously transferred inoculum was added to 45 mL of LB broth with a specific amount of CIP and incubated for at 37°C with shaking at 150 rpm for another 12 hours. This transferring step was repeated for a total of 15 times, as shown in **Figure 3.4**, and a negative control with LB broth alone was always included. The population increased with approximately 3 generations of bacteria per transfer.

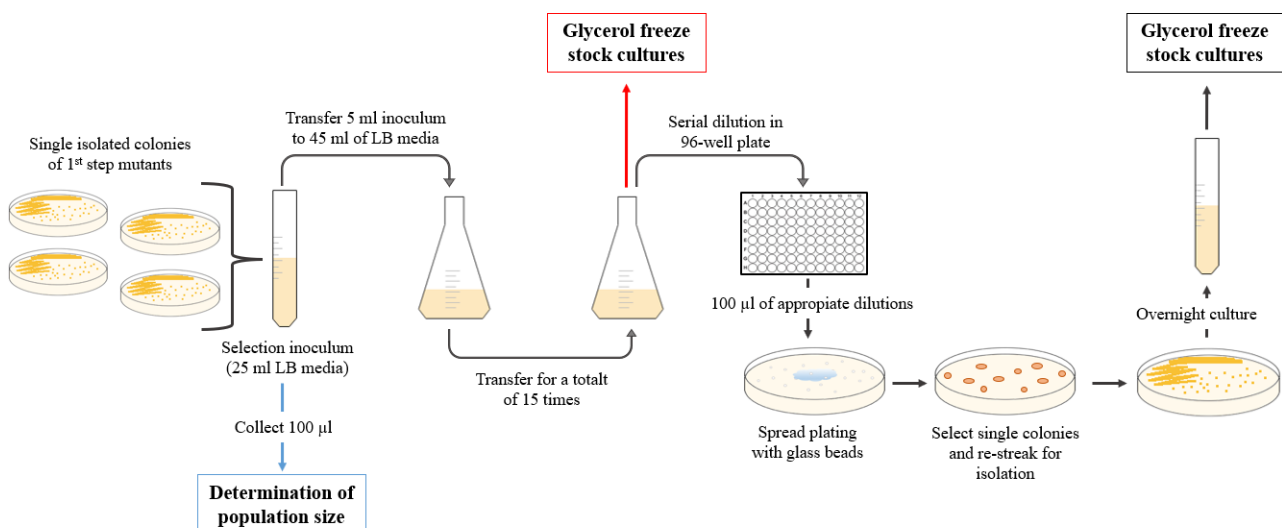


Figure 3.4: A schematic illustration of the dynamic selection method

Finally, portions of the inoculum were used to prepare glycerol freeze-stocks (see **Section 3.3.3**), some of the remaining bacterial media was diluted and 100 µl of appropriate dilutions were plated on non-selective MHA plates to obtain single isolated colonies. For every strain, 5 mutants of interest with varying colony sizes, where chosen. These were separately re-streaked for isolation on non-selective MHA plates and incubated overnight 37°C. An overnight culture was prepared the following day, by selecting one single colony and suspending it in LB broth. After incubation overnight at 37°C with 150 rpm shaking, freeze-stocks were prepared and stored at -80°C for further study.

3.5.4 Calculating populations size of the initial inoculum

A 100 µl sample of the initial selection inoculum was collected for determination of selection population size prior to the first transfer. The dilution and plating was executed as described in **Section 3.4.3**. Inoculated plates were incubated at 37°C overnight before CFU were counted for each dilution plate and used to calculate the cell density per mL as well as the total number of cells per selection inoculum.

Cell density per mL was calculated by multiplying the dilution factor with the number of counted colonies:

$$\text{Cell density per ml} = \text{dilution factor} \times \text{counted colonies dilution plate} \left(\frac{\text{CFU}}{1000 \mu\text{l}} \right)$$

The total number of cell per selection inoculum was further determined by multiplying the cell density per mL with the total transferring volume of 5 mL.

3.6 Isolation of genomic DNA

DNA was isolated using the GenElute Bacterial Genomic DNA Kit (Sigma Aldrich, USA), which allows for extraction of high quality DNA. All necessary reagents not provided in the kit, such as the Lysozyme Solution and Proteinase K Solution, were assembled separately according to the manufacturer's manual.

Prior to the isolation process, inoculums of the bacterial isolates of interest were prepared in MH broth (see **Section 3.3.2**) and incubated over night at 37°C with shaking at 150 rpm. The following day, cells were harvested by pelleting 1,5 mL of the overnight culture at 13 000 rpm for 2 minutes. The supernatant was discarded and the pellets were thoroughly re-suspended in 200 µl of 45 mg/mL Lysozyme solution and placed in the incubator at 37°C for 30 minutes.

After incubation, 20 µl of the RNase A solution was added to each sample and incubated at room temperature for 2 minutes. Then 20 µl Proteinase K solution and 200 µl Lysis Solution C was added and afterwards the samples were vortexed and placed in a heating block at 55°C for 10 minutes. During the incubation time, pre-assembled GenElute Miniprep Binding Columns

were placed in 2 mL collection tubes and prepared by adding 500 µl of the Column Preparation Solution and centrifuged at 13 000 rpm for 1 minute before discharging the elute.

To prepare the lysate for binding, 200 µl of 98% ethanol was added and thoroughly mixed by vortexing for 15 seconds. The entire sample was then transferred to the binding column, centrifuged at 13 000 rpm for 1 minute and the elute was discharged. Then 500 µl of Wash Solution 1 was added to each of the columns and centrifuged for 1 minute at 13 000 rpm. The collection tubes containing the elute were then replaced and 500 µl of the Wash Solution was added for the second wash. The samples were centrifuged at 13 000 rpm for 3 minutes, the elute removed, then an additional one minute at 13 000 rpm to remove residual ethanol. For the final steps, the columns were transferred to new collection tubes, and the DNA was eluted by adding 100 µl of the Elute Solution, followed by incubation at room temperature for 5 minutes and centrifugation for 1 minute at 13 000 rpm. Quality and quantity of the isolated DNA were determined by Nanodrop analysis before storing the samples at -20°C.

3.6.1 Determination of DNA quality and quantity with NanoDrop

A Nanodrop analysis provides useful information about the DNA samples in terms of quantity, given in ng/µl, in addition to purity expressed through the ratios A260/280 and A260/230. The 260/280 ratio is used as an indication of contaminants (such as phenol or protein) that absorbs around 280 nm, while the 260/230 ratio measures other contaminants that absorb at 230 nm. Uncontaminated and high-purity DNA samples should generally have 260/280 ratios around 1,8 and the values for 260/230 ratios should be expected in the range of 2,0 - 2,2. For extracted DNA samples with concentrations below 50 ng/µl the DNA isolation process was repeated.

A small portion of the extracted DNA was analyzed using a Nanodrop spectrophotometer (Thermo Fisher Scientific) to determine the concentration and purity of the sample. A small sample of Milli-Q water was applied to clean the spectrophotometer, then the Elute Solution from GenElute Bacterial Genomic DNA Kit was used to blank the apparatus before 1,5 µl of each DNA sample was loaded and measured separately.

3.7 Polymerase Chain Reaction

Polymerase chain reaction (PCR) is an *in vitro* technique used to amplify specific regions of DNA. In this project, Phusion High-fidelity DNA polymerase (New England BioLabs, USA)

was used to amplify regions of the *gyrA* and *parC* genes from the isolated genomic DNA samples (see **Section 3.6**) to enable detection of genetic variations causing CIP resistance. In addition to the enzyme and DNA template, reagents such as specific primers, dNTPs (nucleotides) and DNA polymerase enzyme were also required for the reaction. Primers used in this project, in both PCR and sequencing reactions, are listed in **Table 3.5**.

Table 3.5: Overview of primers used for amplification of *gyrA* and *parC* genes

Gene	Primer name	Oligonucleotide sequence (5' to 3')	Annealing temperature	Expected band size
<i>gyrA</i>	GyrAR1000	GAGCGCGGATATACACCTT	53°C	680
	GyrAFQ322	GAGCTCCTATCTGGATTAT		
<i>parC</i>	ParCR981	GTGGTAGCGAAGAGGTGGTT	65°C	875
	ParCFQ107	GACCGTGCGTTGCCGTTTAT		

The PCR samples were prepared by assembling a master mix using the components listed in **Table 3.6**. The reagents were added in the same order as listed, then mixed thoroughly and aliquoted into smaller volumes, before adding the genomic DNA templates. The volume of genomic DNA was calculated with results from a Nanodrop analysis (see **Section 3.6.1**). In addition to the PCR-samples containing genomic DNA, a negative control sample was always included and later used in the gel electrophoresis (see **Section 3.8**) to exclude potential contamination.

Table 3.6: Components of PCR samples

Reagents	Stock concentration	Volume	Final concentration
Milli-Q water		q.s. 40 µl	
Phusion High Fidelity Buffer	5X	8 µl	1X
dNTP	10 mM	0,8 µl	0,2 mM
Primer 1 (forward primer)	10 µM	2 µl	0,5 µM
Primer 2 (reverse primer)	10 µM	2 µl	0,5 µM
Phusion High fidelity DNA polymerase	2000 U/mL	0,4 µl	0,8 U/reaction
Genomic template DNA			400 ng

The samples were then run through a reaction on a thermal cycler (Marshall Scientific) with the settings listed in **Table 3.7**. During the initial denaturation, double stranded DNA denatures

into two single stranded DNA-templates. Then follows the annealing step, which involves annealing of the primers to complementary single stranded DNA in the target region; a highly temperature-dependent process where the ideal temperature for each primer may vary. In the final step, primer extension, the polymerase enzyme generates a new DNA strand complementary to the single strand, hence creating a new piece of double stranded DNA. Repeating these steps for multiple cycles are often necessary to generate an adequate number of copies of the DNA target for detection and downstream processes.

Table 3.7: Settings for PCR with Phusion High-fidelity DNA polymerase

Step	Description	Temperature	Time
1	Initial denaturation	98°C	30 seconds
2	Denaturation	98°C	10 seconds
3	Annealing	53°C / 65°C	20 seconds
4	Primer extension	72°C	1 minute
5	Repeat steps 2-4 for 29 cycles		
6	Final extension	72°C	10 minutes
7	Hold	10°C	Forever

3.8 Agarose gel electrophoresis

Agarose gel electrophoresis was performed for PCR products in order to exclude potential DNA contamination and confirm desired amplified products based on size. In the electrical field, the negatively charged DNA wanders towards the positively charged electrode. Smaller fragments move easier through the gel matrix than larger fragments, further allowing for size separation. Added ethidium bromide (EtBr) intercalates with the DNA samples, making them visually detectable under ultraviolet (UV) light.

The 1% agarose gel was prepared by dissolving 0,5 g of agarose (SeaKem, USA) in 50 mL of 1X TAE-buffer by carefully heating the mixture to the boiling point in a microwave. Then 25 µl of EtBr was added and carefully mixed, and the solution was poured into an appropriate casting tray and left to solidify at room temperature for approximately 20 minutes. After transferring the solidified agarose gel to an electrophoresis chamber, a necessary amount of 1X TAE buffer was added to cover the gel surface. The samples, prepared by combining 2 µl of a 6X loading dye with 10 µl of the PCR product, were pipetted into separate wells of the gel. In

addition to the PCR-samples containing genomic DNA, a negative control sample was also included. A 5 μ l sample of Smart Ladder (Eurogentec, Belgium) was loaded into the first and last well of each gel, later used as a tool for size determination of fragments. Gels were run at 90 volts for 35 minutes.

3.9 DNA sequencing

The BigDye terminator v3.1 cycle sequencing kit (Thermo Fisher Scientific) was used to sequence short DNA strands previously amplified through PCR and determine the order of nucleotide bases. The samples for DNA sequencing were prepared by combining the reagents listed in **Table 3.8**, followed by a reaction in a thermal cycler with the settings: 98°C for 1 minute, then 25 cycles of 96°C for 10 seconds; 50°C for 5 seconds and 60°C for 2 minutes. Separate reactions were setup for sequencing in the forward and reverse direction, using the same primers as for the PCR reactions (listed in **Table 3.5**).

Table 3.8: Components of the DNA sequencing sample

Reagents	Volume
DNA template	2 μ l
10 μ M Primer (either forward or reverse)	0,5-1 μ l
5X Big Dye Sequencing Buffer	4 μ l
Big Dye v3.1	1-2 μ l
Sterile Milli-Q water	Ad. 20 μ l

The prepared sequencing samples were analyzed at the Medical Genetics Department at UNN in Tromsø. The obtained data was assembled and interpreted using Sequencher (version 5.3, Gene Codes Corporation, USA), a software program that allows for analysis and comparisons of DNA sequences. In order to detect any nucleotide discrepancies in the *gyrA* and *parC* genes, comparisons were made between the parental wild type strain and their respective mutants.

3.10 Antimicrobial susceptibility testing

Antimicrobial susceptibility testing was performed by MIC-testing with diffusion strips and determination of fold increase in IC₉₀. While the minimal inhibitory concentration (MIC) measures the lowest concentration of an antimicrobial agent that inhibits visible growth of the organism, the IC₉₀ values measure the concentration necessary to inhibit $\geq 90\%$ of the growth.

3.10.1 Minimal inhibitory concentration with diffusion strips

MIC values of the generated CIP mutants were determined using CIP and temocillin (TMO) diffusion gradient strips (Liofilchem, Italy). The results were used to confirm clinical resistance towards CIP by comparison to the EUCAST clinical breakpoint. MIC values below the breakpoint were interpreted as sensitive, while values above were interpreted as resistant. TMO was included to allow exclusion of mutants with potential efflux-pump mediated resistance.

Prior to MIC testing, the mutant of interest, parental WT and the control strain (ATCC 25922) were struck for isolation on non-selective MHA plates (see **Section 3.3.1.1**) and incubated overnight at 37°C. The following day, using a sterile cotton swab, small amounts of the isolated colonies were re-suspended in glass tubes containing 85% saline solution and adjusted the optical density to that of a 0,5 McFarland ($\approx 1,5 \times 10^8$ CFU/mL), measured with a calibrated densitometer. Within 15 minutes of preparation, a new cotton swap absorbed in the bacterial suspension was used to inoculate a MHA plate with the swab plating technique (see **Section 3.3.1.3**).

The plate(s) were left to dry for a maximum of 15 minutes, before application of the MIC-strips with sterilized forceps. After application, sterile toothpicks were used to gently press the strips against the surface of the agar, while avoiding any movement of the strips, to remove potential air-bubbles and gaps. The plate(s) were then incubated at 37°C for 18 hours before MIC values were read directly from the scale, at the point where the elliptical inhibition zone intersected with the strip.

3.10.2 IC₉₀ determination

The IC₉₀ was determined by performing a serial 1,5-fold dilution of six antimicrobial agents (listed in **Table 3.9**) to investigate increased or reduced sensitivity of the isolated CIP resistant mutants.

Table 3.9: Overview of antimicrobial agents included for IC90 testing

Antimicrobial agent	Antimicrobial class	Antimicrobial target
Ceftazidime (CAZ)	β -lactams	Cell wall synthesis
Chloramphenicol (CHL)	Amphenicols	Protein synthesis
Ciprofloxacin (CIP)	Fluoroquinolones	Nucleic acid synthesis
Colistin (COL)	Polymyxines	Cell membrane function
Gentamicin (GEN)	Aminoglycosides	Protein synthesis
Trimethoprim (TMP)	Antifolates	Folic acid synthesis

Isolates of interest, their parental WT strain and the control strain (ATCC 25922) were struck for isolation on non-selective MHA plates (see **Section 3.3.1.1**) and incubated overnight at 37°C. The following day, a 0,5 McFarland suspension was prepared for each isolate by re-suspending colonies from the MHA plates in an 85% saline solution. The McFarland suspension was further diluted 1:1000 in MHB. Normally, 5 μ l of the McFarland suspension was added to 4,995 mL of MHB in a falcon tube and mixed by inverting the tube 20-30 times.

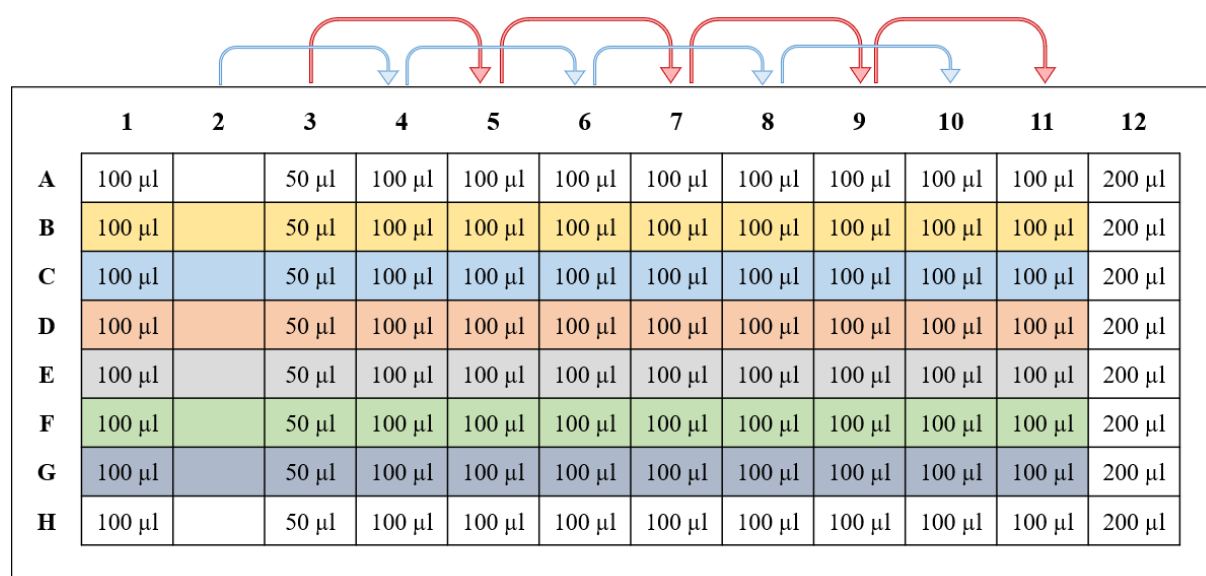


Figure 3.5: A schematic illustration of 1,5-fold dilution in a 96-well plate

A 96-well plate was prepared by adding a specific amount of MHB (volume added to each well is shown in **Figure 3.5**). The working stock of the antimicrobial drugs were diluted in MHB to double the highest tested concentration. Drugs were further added to two of the columns; 200 μ l of the drug was added to the column 2 and 150 μ l of the same drug was added to column 3,

following mixing by pipetting 12 times. The dilution of the antimicrobial in the 96-well plate was performed in two separate series, in the first series 100 µl was transferred from column 2 to column 4 and mixed thoroughly by pipetting 12 times. This was continued for every second well across the plate, as illustrated with the blue arrows in **Figure 3.5**. For the second series, dilutions were performed in a similar manner starting from column 3 and transferring to every second well across the plate, as illustrated by the red arrows in **Figure 3.5**. Pipetting tips were changed between each series and 100 µl was discarded from the final well of each dilution series.

Following the serial dilution, 100 µl of the prepared bacteria inoculate was added to column 1-11, adding the same strain in each row starting from the second row, as highlighted in **Figure 3.5**. The control strain, ATCC 25922, was always included for each drug and in each plate tested. Only bacteria were added to column 1, the positive control, and neither bacteria nor drug was added to column 12, as these were the negative controls. The 96-well plate(s) were incubated at 37°C with shaking at 700 rpm for 18 hours. After incubation, the absorbance at 600 nm ($A_{600\text{nm}}$) was measured using a plate reader (Molecular Devices).

The IC_{90} values were calculated using the absorbance at 600 nm ($A_{600\text{nm}}$) measurements of the strain, the negative and positive control, with the following equation:

$$\% \text{ inhibition} = \left(1 - \frac{A_{600} \text{ drug treated} - A_{600} \text{ negative control}}{A_{600} \text{ positive control} - A_{600} \text{ negative control}} \right)$$

Testing was repeated if values for the control strain were out of the expected range. Fold changes were calculated by comparison of the mutant to the wild types with the same drug using one of the following equations, based on if whether CS or CR was observed:

$$\text{Fold change (CR)} = \frac{\text{Mutant } IC_{90}}{\text{WT } IC_{90}}$$

$$\text{Fold change (CS)} = - \frac{\text{WT } IC_{90}}{\text{Mutant } IC_{90}}$$

4 Experimental results and discussion

The aim of this study was to generate CIP resistant isolates from clinical *E. coli* strains, with mutations to the *gyrA* and *parC* genes confirmed with DNA sequencing. The CR/CS patterns of selected CIP resistant isolates were determined by IC₉₀ testing and results were compared to the parental isolates. Experimental results are presented and discussed in the sections below.

4.1 *E. coli* isolates clinically resistant to ciprofloxacin

CIP resistant mutants were spontaneously evolved using two distinct methods from three clinical *E. coli* strains selected from the ECO-SENS study. We aimed to generate isolates with mutations to the *gyrA* and *parC* genes as these mutations are most prevalent in clinical strains (44, 45). Antimicrobial gradient diffusion strips were used to confirm resistance to CIP. Isolates with MIC values above 0,5 µg/mL, the EUCAST clinical breakpoint for CIP, were considered clinically resistant. MIC values were also determined for temocillin (TMO). MICs for TMO considerably greater than the parental WT was used as an exclusion criteria in this study, as reduced susceptibility to TMO resistance has been associated with efflux-pump mediated resistance, as previously observed by Podnecky et al (42).

4.1.1 Isolates generated through the static selection method

Through the static selection method, resistant mutants were generated stepwise with a gradual increase in selection concentration (see **Section 3.4**). This process generally required multiple selection steps. In the first step, considerable amounts of growth on selective plates with the concentrations 0,032 µg/mL and 0,064 µg/mL were observed for all strains, in addition to dense growth on lower concentrations. Growth on 0,128 µg/mL was observed solely for the K56-12 strain. For each strain, ten single colonies generally “healthy” looking (visually large and circular) were chosen for further study (**Appendix A**). The isolates were purified from various selection concentrations, as highlighted in **Figure 4.1**.

The calculated average mutation frequency for the first selection step was highest for the K56-12 strain and lowest for K56-78 strain, at $1,1 \times 10^{-8}$ and $7,8 \times 10^{-9}$, respectively. All isolates had a significant increase in resistance to CIP, however, values larger than or equal to the clinical breakpoint were only observed for six mutants, generated from the K56-12 and K56-78 strains,

as shown in **Figure 4.1**. None of the mutants evolved from the K56-2 strain were clinically resistant to CIP at this point. MICs for CIP ranged from 0,19 to 0,5 $\mu\text{g}/\text{mL}$, with great variation within each strain. Compared to the MIC values of their corresponding parental strain (**Appendix B**), no mutants displayed reduced susceptibility to TMO.

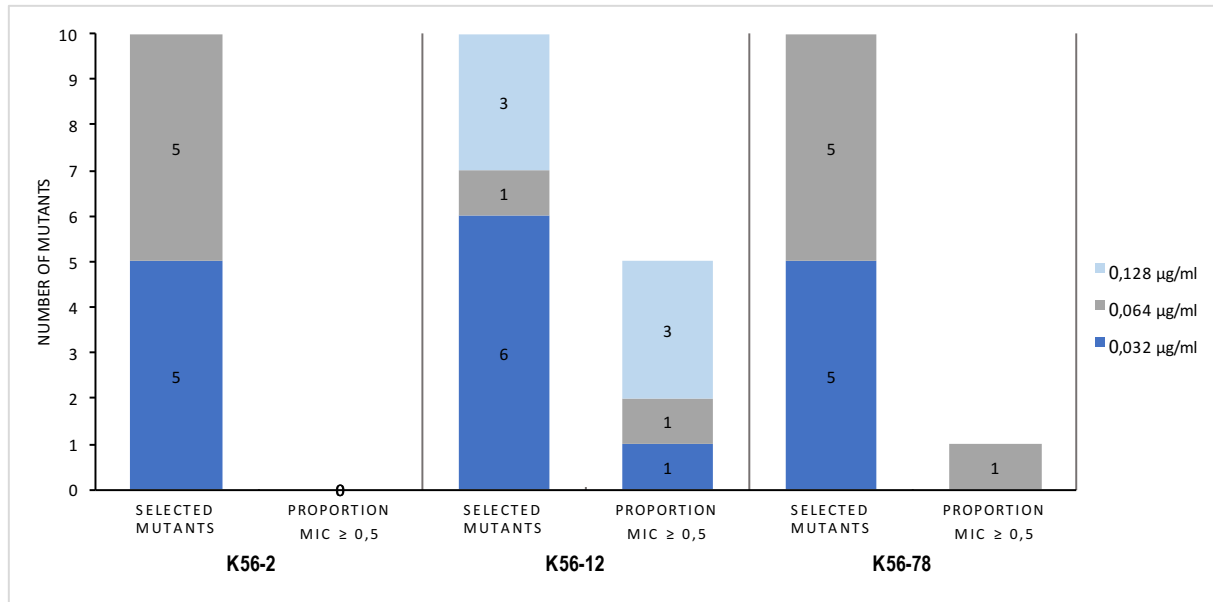


Figure 4.1: An overview of selection concentration and mutants with CIP MIC \geq the clinical breakpoint for first step mutants sorted by parental strain

A secondary selection with increased concentrations of CIP (0,25 $\mu\text{g}/\text{mL}$ and 0,5 $\mu\text{g}/\text{mL}$) was performed using the first step isolates, in order to achieve higher levels of CIP resistance and the desired mutations. A considerable amount of growth was observed at both concentrations, with the exception of two of the K56-78 mutants (first step mutants #8 and #4, **Appendix A**) which showed no growth. Multiple colonies were isolated from each strain, listed in **Appendix C**. The highest average mutation frequency at $2,2 \times 10^{-7}$ was observed for the K56-2 mutants, while the K56-78 mutants showed lowest frequency at $1,3 \times 10^{-9}$. All mutants had CIP MICs above the clinical breakpoint and a simultaneous increase in MICs for TMO compared to the first-step isolates (**Appendix A**).

Following the second step selection, several unsuccessful attempts were made to generate third-step mutants at the CIP concentrations of 1 $\mu\text{g}/\text{mL}$, 4 $\mu\text{g}/\text{mL}$ and 8 $\mu\text{g}/\text{mL}$. On multiple occasions and with several growth media (MHA from two distinct manufacturers and LBA) growth was only observed for the K56-2 strain on 1 $\mu\text{g}/\text{mL}$. These isolates were originally purified and intended for further study. However, they were eventually excluded upon MIC-

testing due to reduced TMO susceptibility, values ranged from 32 to 64 $\mu\text{g}/\text{mL}$, and nearly unaltered level of CIP resistance of 2 $\mu\text{g}/\text{mL}$, compared to previous second-step isolates (**Appendix D**).

Additionally, a few promising second-step isolates, generated from the K56-12 strain, were selected for sequencing. These isolates displayed high levels of CIP resistance (MICs ranged from 1 to 1,5 $\mu\text{g}/\text{mL}$) and a relatively small decrease in susceptibility to TMO relative to their parental WT strain (MICs ranged from 8 to 24 $\mu\text{g}/\text{mL}$). A point mutation in *gyrA*, S83L, was identified in all sequenced mutants, but no mutations were identified in *parC* (**Appendix E**). With this knowledge and the observed reduced susceptibility to TMO, we presumed that the majority of the second step mutants had an efflux-pump mutation and lacked a desired mutation to the *parC* gene without further sequencing.

4.1.2 Isolates generated through the dynamic selection method

Due to the presumed absence of *parC* mutations in all isolates selected at higher CIP concentrations through the static method, explained by the reduced sensitivity to TMO, a second approach was attempted in order to generate such mutations (see **Section 3.5**). The dynamic method involved selection in liquid growth medium with shaking during incubation and serial transfers to fresh medium. This approach was chosen based on a previous study, where the authors had successfully selected CIP resistant *E. coli* isolates with *parC* mutations (45). In this study, the majority of their selected isolates (18/20 mutants) had acquired GyrA mutations followed by a ParC mutation (45).

We used the dynamic selection method to evolve second-step mutants from the statically selected first-step mutants (**Appendix A**) under a lower constant antimicrobial pressure. Without prior sequencing of all generated first-step mutants, an assumption was made that all isolates carried a *gyrA* mutation. This assumption was based on the sequencing results of some statically selected second-step mutants (**Appendix E**), low TMO MIC values and previous studies suggesting that first-step mutations following exposure to CIP are typically found in *gyrA* (45, 47). The selection concentrations were 0,5 \times the MIC value, based on the average values MIC values of the mutants within each strain. Two parallel transfers in two separate flasks were performed for each strain. The total population size of each transfer was

approximately 1×10^{10} cells per flask, and overall 45 generations were achieved through a total of 15 transfers.

Following serial passage, five mutants from each strain were selected and isolated, listed in **Table 4.1**. Mutants selected from the same flasks, separated by the dotted lines in **Table 4.1**, were expected to have the same mutations and therefore similar MICs. MIC testing confirmed clinical resistance to CIP in the majority of isolates, with observed MICs ranging from 0,38 to 8 $\mu\text{g/mL}$, similar to the second-step mutants generated through static selection (**Appendix C**). In total, 14 of 15 isolates were defined as clinically resistant to CIP as defined by the EUCAST breakpoint. A small increase in TMO resistance was observed for several of the mutants. However, these values were generally lower and closer to the WT strains compared to previous second step isolates, which suggested a reduced rate of efflux-pump mediated resistance mutations. All 15 mutants were included for further study.

Table 4.1: Overview of second step mutants generated through dynamic selection at sub-MIC selective concentration

Parental isolate	Selection population size	Mutant #	Selection concentration CIP ($\mu\text{g/mL}$)	Approximate colony size, diameter (mm)	MIC CIP ($\mu\text{g/mL}$)	MIC TMO ($\mu\text{g/mL}$)
K56-2	$1,1 \times 10^{10}$	P1-1	0,176	2	1,5	6
		P1-2	0,176	2	1,5	6
		P2-1	0,176	0,5	1	8
		P2-2	0,176	2	8	6
		P2-3	0,176	1,5	1	6
K56-12	1×10^{10}	P1-1	0,194	2	0,75	8
		P1-2	0,194	2	1	12
		P2-1	0,194	0,5	0,75	8
		P2-2	0,194	1,5	1	8
		P2-3	0,194	0,5	0,5	8
K56-78	$1,3 \times 10^{10}$	P1-1	0,158	2	0,5	4
		P1-2	0,158	0,5	0,38	8
		P2-1	0,158	1,5	0,75	4
		P2-2	0,158	1,5	0,75	4
		P2-3	0,158	0,5	0,75	4

4.2 Identified variations in resistant isolates

4.2.1 PCR amplification and agarose gel electrophoresis of *gyrA* and *parC*

PCR was used to amplify the specific regions of interest, with high-quality DNA isolated from the CIP resistant mutants of interest. The parental WT strains were also included for later comparisons. Prior to sequencing, the PCR products were visualized on an agarose gel to confirm that correct regions were amplified during the reaction. Migration distance in comparison to the smart ladder (**Appendix F**) was used to approximate the size of each PCR product, which was compared to expected band size of the desired products (listed in **Table 3.5**).

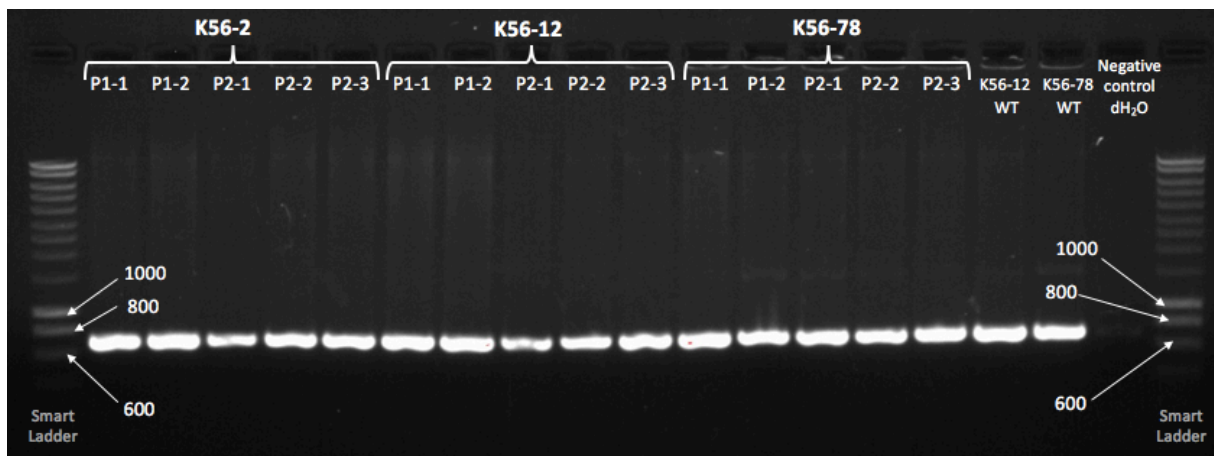


Figure 4.2: Gel image of *gyrA* amplified PCR products

PCR amplified *gyrA* products yielded single bands between 600-800 base pairs for all tested isolates, consistent with the positive *gyrA* control strain (680 base pairs), as shown in **Figure 4.2**. Similarly, shown in **Figure 4.3**, all *parC* products were observed between 800-1000 base pairs for all testes isolates, consistent with the positive *parC* control strain (875 base pairs). Following no observation of additional and unexpected bands, the samples were prepared and sent for DNA sequencing.

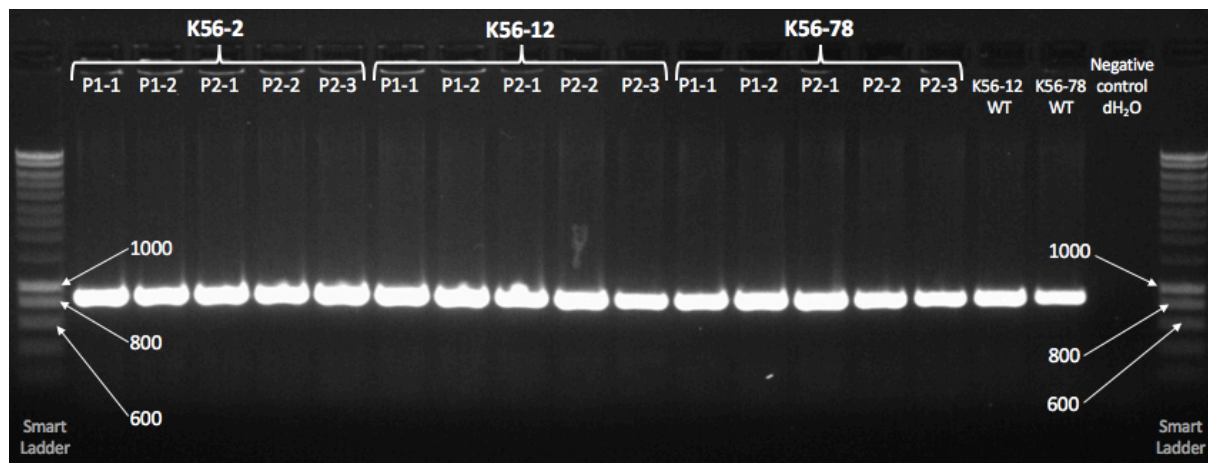


Figure 4.3: Gel image of *parC* amplified PCR products

4.2.2 Identified point mutations with sequence data

Mutations were identified by comparisons of the WT parental strain sequence and sequences of their respective mutants (**Appendix G**). During initial sequencing reactions, we encountered some problems when sequencing for *parC* mutations, due to poor sequencing quality. Despite the quality, we were initially able to compare significant regions of the sequence and identified putative variations in the DNA sequence. However, the sequencing quality of the isolates K56-12 P1-2 and K56-78 P1-1 was so poor that the chromatographs could not be properly aligned to the WT reference sequence. All nucleotide discrepancies identified in *gyrA* and *parC* between the parental WT strain and their corresponding mutants, listed in **Table 4.2**, were characterized as SNPs with a nonsynonymous effect.

In order to improve the *parC* sequencing quality, the amount of BigDye and sequencing primers was doubled (see **Table 3.8**). Re-sequencing of *parC* showed improved quality and the previously identified mutations were confirmed, in addition to revealing mutations in K56-12 P1-2 mutant and K56-78 P1-1 mutant (listed in **Table 4.2**). However, K56-12 P1-2 and K56-78 P1-1 were not included for further testing and IC₉₀ determination since promising mutants had already been selected based on the preliminary sequencing data.

Table 4.2: Overview of identified mutations in CIP resistant mutants

Parental isolate	Mutant #	<u>GyrA</u>		<u>ParC</u>	
		Nucleotide mutation	Amino acid mutation	Nucleotide mutation	Amino acid mutation
K56-2	P1-1	248 C→T, 260 A→G	S83L, D87G	232 G→T	G78C
	P1-2	248 C→T, 260 A→G	S83L, D87G	232 G→T	G78C
	P2-1	248 C→T	S83L	239 G→T	S80I
	P2-2	248 C→T, 260 A→G	S83L, D87G	250 G→A	E84K
	P2-3	248 C→T	S83L	250 G→A	E84K
	K56-12	P1-1	248 C→T	S83L	250 G→A
P1-2		248 C→T	S83L	233 G→A*	G78D*
P2-1		248 C→T	S83L		
P2-2		248 C→T	S83L	233 G→A	G78D
P2-3		248 C→T	S83L		
K56-78		P1-1	248 C→T	S83L	238 A→C*
	P1-2	248 C→T	S83L		
	P2-1	248 C→T	S83L	235 G→A	D79N
	P2-2	248 C→T	S83L	235 G→A	D79N
	P2-3	248 C→T	S83L	235 G→A	D79N

* Additional *parC* mutations identified during re-sequencing, not included in the IC₉₀ testing

4.2.2.1 GyrA

Mutations in *gyrA* were identified in all 15 dynamically selected mutants. The S83L mutation was identified in all isolates, which is consistent with the assumption that mutants selected from the same flasks would have the same mutations. However, additionally three of five isolates of the K56-2 strain carried mutations altering the aspartic acid in position 87, a variation which no other strains displayed. Both mutations have previously been reported in fluoroquinolone resistant *E. coli* isolates (44, 48, 49). Although the S83L mutation appears to emerge more frequently than any other GyrA mutation, this single mutation alone gives low level CIP resistance in comparison to a combination of S83L and a substitution of the aspartic acid in position 87, which often gives higher levels of resistance (47). The increased level of resistance in isolates carrying two diverse mutations in GyrA is also observed in our MIC data (**Table 4.1**, **Table 4.2**) where the highest MICs were observed for the K56-2 mutants with both the S83L and D87G mutation.

4.2.2.2 ParC

Overall, ParC mutations were identified in overall 12 of 15 isolates. All five mutants from the K56-2 strain background had variations to the *parC* gene. In the remaining strains *parC* mutations were identified in four of five K56-78 isolates and in three of five K56-12 isolates. This may suggest that *parC* mutations occur more easily or frequently in the K56-2 strain than the K56-12 and K56-78 strains, since the only isolate with a *parC* mutation from previous studies of the MicroPop research group was generated from K56-2 (42).

The majority of identified ParC mutations (G78C, S80I, E84K, S80R and G78D) have previously been found in CIP resistant *E. coli* isolates with the exception of the D79N mutation, which was found in three of five K56-78 isolates (42, 45, 50). However, substitution of the aspartic acid in position 79 with alanine has previously been reported (45). Overall, the most frequently observed ParC mutation in our isolates was the E84K mutation, identified in two of the strains. A previous study using the same selection approach found several mutations to the glutamic acid in position 84, but overall the most frequently identified mutation in their strains was the S80I mutation (45). The S80I mutation was only found in one of our isolates, the K56-2 P2-1 mutant.

Variation in ParC mutations was found in the same passage within each strain; although we expected the same mutations and similar MICs in isolates selected from the same flasks. In the K56-2 P1 isolates and the K56-78 P2 isolates, the same ParC mutations were identified (see **Table 4.2**), suggesting that these mutations were able to outcompete other mutations during the selection process. Similar MICs were also measured for these isolates (see **Table 4.1**). However, we also observed that isolates with the same ParC and GyrA mutations, such as the K56-12 P1-2 and P2-2, had dissimilar MICs for CIP and TMO, which is inconsistent with our initial assumption.

Isolates lacking *parC* mutations were suspected to have resistance acquired through other mechanisms, such as efflux and/or porin related mutations. In K56-78 1-2, we observed reduced susceptibility to TMO and low-level CIP resistance. Increased CIP resistance in this particular isolate could be explained by an efflux related mutation or simply due to the single *gyrA* mutation. In the two other isolates, K56-12 2-1 and 2-3, no increased TMO MICs were observed, increased CIP resistance in this case are presumably caused by other resistance mechanism rather than efflux. However, without further investigation we were not able to confirm that resistance is caused by either of the mentioned mechanisms.

4.2.3 CIP resistance evolution in *E. coli* isolates

We observed during our selection process that resistance development to CIP in *E. coli* isolates usually required multiple mutations to reach higher levels of resistance. Similarly, it has been shown that at least two distinct mutations are required to reach MIC of CIP > 4 µg/mL, but one *gyrA* mutation alone may contribute to resistance above the CIP clinical breakpoint (50). A proposed experimentally-supported mathematical model illustrating the mutational evolution in CIP resistant *E. coli*, suggests that there is one main trajectory leading to clinically relevant resistance (45). This main trajectory starts with the acquisition of a GyrA mutation (S83L), followed by a ParC mutation (S80I) and lastly a secondary mutation to GyrA (D87N).

The assumption that the acquisition of GyrA mutations generally occurs prior to the ParC mutations, due to the fact that DNA gyrase in Gram-negative bacteria is more susceptible to quinolones, further supports this evolutionary model (33). However, without sequencing data from in-between selection steps, we are not able to determine which GyrA mutations was first acquired in our isolates of the K56-2 strains carrying both the S83L and D87N mutation.

Previous studies have found that strains containing the S83L mutation are able to outcompete any alternative GyrA mutation and that it is initially the most frequently found mutation (45, 47). We can assume that these findings also apply to our isolates and that the acquisition of the S83L mutation occurred prior to any other mutation.

The second mutation acquired in most of our isolates from the K56-2, K56-12 and K56-78 strain background that carry two mutations, was the ParC mutation. MICs of these isolates are consistent with previously observed values of isolates carrying a single GyrA and ParC mutation, ranging between 0,25 and 2 $\mu\text{g/mL}$ (45, 47, 50). For the K56-12 isolates that carry three mutations, the secondary occurring mutation could either be the ParC mutation or another GyrA mutation (D87N), although the model strongly suggests that the ParC mutation generally occurs prior, due to its competitive advantage over the combination of two GyrA mutations (45). MICs of CIP resistant isolates carrying three similar mutations have previously been measured in the range between 16 and 256 $\mu\text{g/mL}$, however, the measured MICs of our isolates with three mutations showed values ranging between 1,5 and 8 $\mu\text{g/mL}$ (45, 50).

4.3 Collateral sensitivity and cross-resistance profiles

Changes in susceptibility to six unrelated antimicrobial agents with diverse mechanisms of action, listed in **Table 3.9**, were determined for the generated CIP mutants with both GyrA and ParC mutations using the IC₉₀ assay. These antimicrobial agents were chosen based on the previous study in the MicroPop research group as we wanted to investigate whether the susceptibility patterns of our CIP resistant isolates with GyrA and ParC mutations were consistent with the observed patterns of CS/CR (42).

4.3.1 IC₉₀ assay

A 1,5-fold dilution of the antimicrobial agents were used to test the isolates with both GyrA and ParC mutations. The parental WT strain and the control strain (ATCC 25922) was also included and the testing was performed once on all strains with each drug. Tests were repeated if the control strain was out of range upon comparison to expected values (**Appendix H**). IC₉₀ values were compared to those of their parental WT strain by calculating the fold change using the measured A₆₀₀ values (**Appendix I**). A heat map illustrating the observed cross-resistance and collateral sensitivity of our isolates was assembled using the calculated fold changes (**Appendix I**). Increased susceptibility or collateral sensitivity was reported with negative

values below 0 (illustrated with the blue color scheme), while decreased susceptibility or cross-resistance was reported with values above 0 (illustrated with the red color scheme). No change in susceptibility was reported as 0.

4.3.2 CS/CR

As expected, a decrease in susceptibility to CIP was observed in all generated isolates with fold changes ranging from 42 to 500. Decreases in susceptibility to CAZ, CHL and COL were also observed for isolates of several strains, as shown in **Figure 4.4**. More specifically cross-resistance to CAZ was observed in five isolates from the K56-2 and K56-78 strain backgrounds, fold changes in these isolates varied from 1,3 to 2. Decreased susceptibility to CHL was observed in two isolates, K56-2 P2-1 and K56-78 P2-2, with fold changes ranging between 1,3 and 1,5. Cross-resistance to COL was observed in three isolates with fold changes ranging between 1,3 to 1,5.

The most interesting observation was the increased susceptibility to GEN observed in the majority of isolates, with the exception of the K56-2 1-2, K56-12 P1-1 and K56-78 P2-3 isolates where no change in susceptibility was observed. Fold changes for GEN sensitivity ranged from -1,33 to -2. However, a decrease in susceptibility to GEN was also observed in one isolate, K56-12 P2-2, with a fold change of 1,33 compared to its WT parental strain. Five isolates in total and at least one isolate from of each strain background also displayed an increased susceptibility to TMP, fold changes where at -1,33 in all cases, as shown in **Figure 4.4**.

Prior to determining the CR/CS patterns in our isolates, we hypothesized that mutants of the same strain carrying the same mutations in GyrA and ParC would display similar susceptibility changes to the same antimicrobial agents. However, K56-2 P1-1 and K56-2 P1-2, which have acquired the same three mutations, show no resemblance in CS and CR with the exception of the evident decrease in susceptibility to CIP. K56-2 P1-1 showed increased susceptibility to GEN, which was not observed in K56-2 P2-1. Likewise, K56-2 P2-1 displayed CS to COL and CR to CAZ, changes that were not observed in K56-2 P1-1.

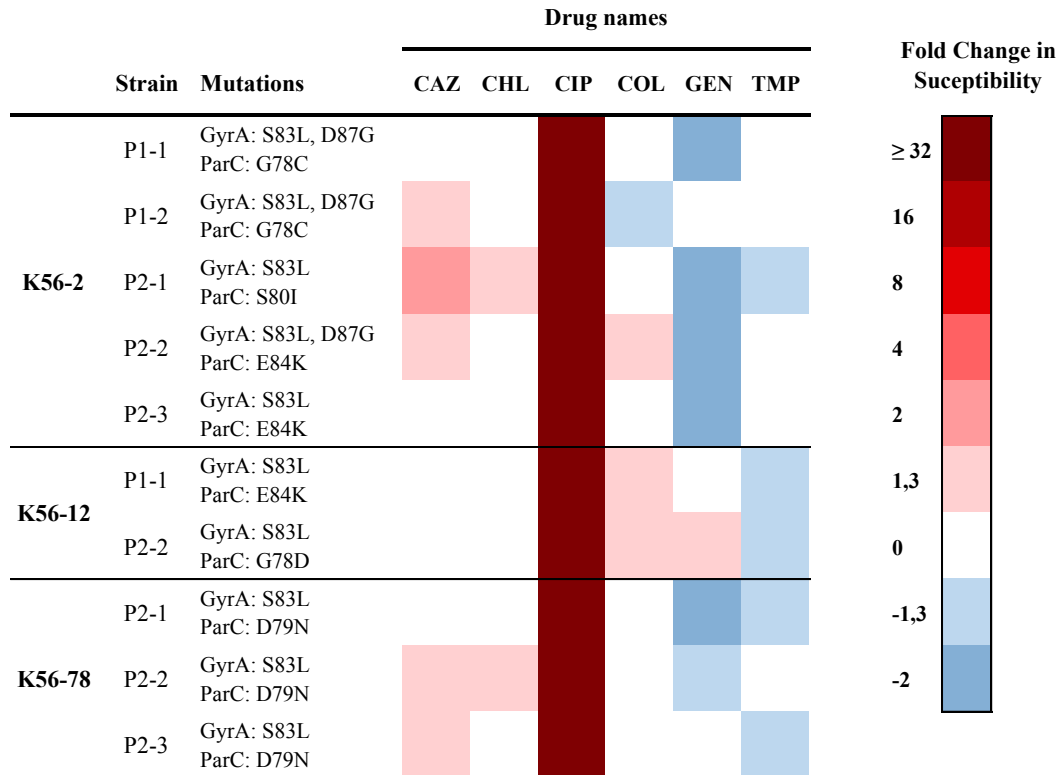


Figure 4.4: Heat map of drug susceptibility profiles of CIP resistant isolates relative to their parental WT strain

Similar mutations were identified in K56-2 P2-3 and K56-2 P2-2, with the exception of an additional mutation to the GyrA gene in the latter isolate. The same level of CS to GEN was observed in both isolates. The K56-2 P2-2 isolate additionally showed CR to COL and CAZ, which were not observed in K56-2 P2-3. This may suggest that the additional CR effects observed is a possible result of the secondary GyrA mutation, D87G.

The mutants K56-2 P2-3 and K56-12 P1-1 were generated from different parental WT strains, but carry the same GyrA and ParC mutations. In K56-2 P2-3 a 2-fold change in CS to GEN was observed, a change in susceptibility that was not observed in K56-12 P1-1. Likewise, K56-12 P1-1 displayed CS towards TMP and CR to COL, changes which were not observed in K56-2 P2-3. A possible reason for the evident differences in observed CS and CR may be related to variation in strain background.

4.3.3 Comparison of CS/CR effects to previous studies

Imamovic and Sommers have previously built complex collateral networks by evolving resistance in *E. coli* to 23 clinically relevant antimicrobial agents and performing IC₉₀ assays on the resistant isolates to determine fold changes in observed CR and CS (41). Our findings from this study are consistent with the described CR to CHL found in their resistant CIP isolate. They observed an 8-fold change in decreased sensitivity compared to the WT strain, whereas a lower fold change ranging from 1,3 to 1,5 was observed in our isolates. However, we also found CS to TMP in several of our isolates from each strain background, and this contradicts with the 32-fold CR effect to TMP described by Imamovic and Sommer. The observed CS to GEN in our tested isolates is inconsistent with the no change in susceptibility observed in their isolates. Imamovic and summer also found no changes in collateral effects to COL, which is inconsistent with the CR to COL observed in our K56-12 isolates and K56-2 P2-2 isolate, and the observed CS found in K56-2 P1-2. We also found CR to CAZ in five of our isolates, but this particular drug was not included or described in their study.

In a study by Lazar *et al.* from 2013, collateral networks were assembled using resistant isolates of *E. coli*, evolved with 12 antimicrobial agents, tested against several other antimicrobials (43). Similarly to our findings, Lazar *et al.* observed a CS effect to GEN in their low-level CIP resistant isolates. However, the CR interaction to CHL found in two of our CIP resistant isolates was not described in their results. Initially Lazar *et al.* found no change in susceptibility to TMP, but in a later study investigating the CR interaction networks, they observed significant CR interactions to TMP, which is inconsistent with the observed CS to TMP found in several of our strain (51). CAZ was not included in either of their studies.

Podnecky *et al.* from 2018 investigated the conserved collateral susceptibility networks of ten diverse clinical strains of *E. coli* to 16 antimicrobial agents in ten diverse clinical strains of *E. coli* (42). Their findings showed a higher prevalence of CR than CS effects in CIP resistant isolates (CIP^R). Sequencing of CIP^R isolates revealed efflux related mutations in nearly all isolates, with the exception of a K56-2 derived isolate which had acquired mutations to GyrA and ParC, as shown in **Figure 4.5**.

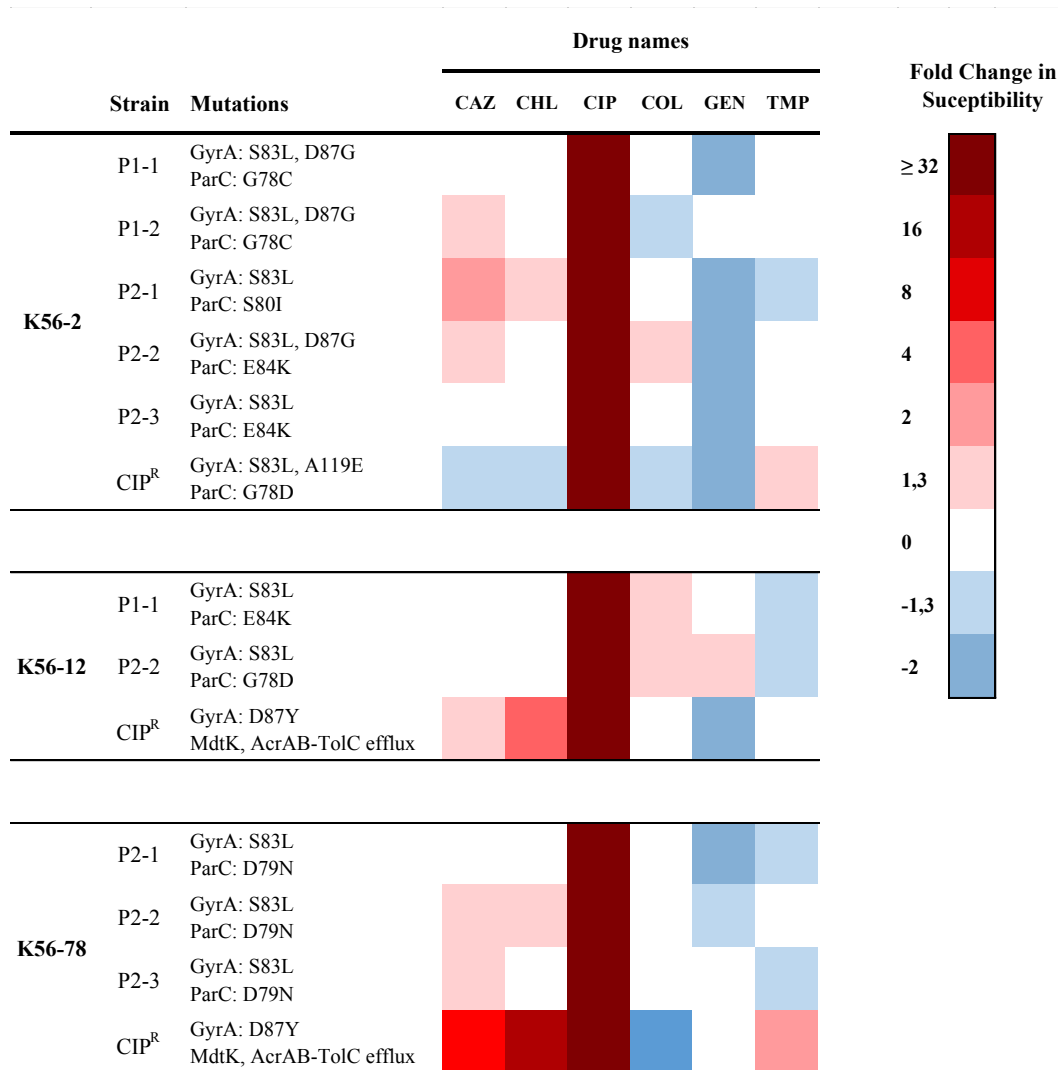


Figure 4.5: Heat map comparing drug susceptibility of our CIP resistant to previous work from Podnecky *et al.* (CIP^R) (42)

In their study, Podnecky *et al.* only showed CS to GEN in the one isolate carrying GyrA and ParC mutations (42). We observed in our study multiple isolates displaying this CS effect. Overall, six of ten CIP resistant isolates showed CS to GEN, as shown in **Figure 4.5**. The K56-2 CIP^R isolate, which is most comparable to our isolates due to its GyrA and ParC mutations, also displayed additional CS effects to CAZ and CHL, which were not observed in any of our isolates. The CS effect observed to TMP in our isolates is also inconsistent with the CR to the same drug found in the K56-2 CIP^R and K56-78 CIP^R mutants. The data presented here suggest that this CS effect is general in *gyrA* and *parC* mediated CIP resistance. A possible reason for the variations in CS and CR observed between our K56-2 isolates and the K56-2 CIP^R mutant may be linked to the variation in point mutations in the *gyrA* and *parC* genes.

Generally, we observed reduced less occurrence of CR with lower fold changes in our CIP resistant isolates generated from the K56-12 and K56-78 strains compared to the CIP^R mutants generated from the same strains by Podnecky et al, as shown in **Figure 4.5**. Our K56-12 isolates only displayed CR to COL and GEN with a 1,3-fold change, while their CIP^R mutant showed a CR effect to CAZ and CHL with fold changes at 1,5 and 4, respectively. Our K56-78 isolates showed CR to CAZ and CHL at a 1,3-fold change. CR to the CAZ and COL was also found in the CIP^R mutant generated from the K56-78 WT strain, in addition to CR to TMP, at higher fold changes ranged from 2 to above 16. The explanation for the increased CR observed by Podnecky *et al.* is suggested to be linked to the multidrug resistance associated with mutations affecting efflux pump expression (42).

4.4 Challenges and limitations of this study

Our study was performed under optimal conditions *in vitro* and may not be conclusively comparable to human physiological conditions. CIP resistant isolates *in vivo* may behave differently depending on acquired mutations or effected by different factors controlling the collateral responses, which in turn can result in variations from the CS and CR profiles observed in this study.

This study is also limited in the sense that the IC₉₀ assay was only performed once on each CIP resistant isolate with each drug, and this could have affected the observed CS and CR profiles. Thus, the IC₉₀ data presented here would need to be repeated to reach publication standard. However, our quality control strain (ATCC 25922) was within the validated ranges. Measurements of our CIP resistant isolates could have been affected by external contamination that did not affect the expected values of the control strain.

5 Conclusion and future prospects

The aim of this study was to evolve CIP resistant *E. coli* isolates with mutations in GyrA and ParC and investigate whether these notations could affect the observed collateral sensitivity and cross-resistance profiles of the resistant isolates. We also wanted to investigate whether CS/CR findings could be associated with the specific mutations or strain background, by comparison to previous studies.

We were able to evolve resistant isolates in three clinical *E. coli* strains with the desired mutations in GyrA and ParC using a dynamic selection method. We identified a variety of point mutations with a nonsynonymous effect, specifically S83L and D87G in GyrA and G78C, S80I, E84K, S80R, G78D and D79N in ParC. We concluded that these mutations contributed to a favorable CS effect to GEN in several isolates of each strain background. This was consistent with previous findings, suggesting that this CS effect might be a general feature of CIP resistant isolates carrying mutations to GyrA and ParC. Additionally, CS effects to TMP were observed, however, this was inconsistent with previous findings. At the same time, our resistant isolates presented CR to several other antimicrobials tested, but we found no clear patterns CR that could be linked to specific mutations or parental strain background. Considering the unpredictable CS/CR patterns alone, we propose that the use of CIP in drug cycling and combination therapy should be carefully considered.

We suggest that more research on CS/CR should be performed prior to exploiting collateral CIP networks in clinical treatment. Our testing was limited to CIP resistant isolates with MICs just above the clinical breakpoint, however, higher levels of CIP resistance and the acquisition of multiple mutations might alter the CS/CS patterns observed. We also propose further research to investigate possible factors contributing to the difficulty of generating CIP resistant isolates with GyrA and ParC mutations *in vitro* using static selection methods, despite these mutations being the most prevalent in CIP resistant isolates *in vivo*. We suggest further investigation of the point mutations identified in GyrA and ParC, to investigate if different combinations would lead to different CS/CR effects. Expanding our knowledge of CS/CR effects in both *in vivo* and *in vitro* CIP resistant isolates and the ability to link these observations to certain mutations, enables prediction of collateral effects and is essential to introducing CS networks in clinical treatment practices.

References

1. Acemoglu D, Johnson S. Disease and Development: The Effect of Life Expectancy on Economic Growth. *Journal of Political Economy*. 2007;115(6):925-85.
2. Davies J, Davies D. Origins and evolution of antibiotic resistance. *Microbiology and Molecular Biology Reviews*. 2010;74(3):417-33.
3. Spring M. A brief survey of the history of the antimicrobial agents. *Bulletin of the New York Academy of Medicine: Journal of Urban Health*. 1975;51(9):1013-5.
4. Lewis K. New approaches to antimicrobial discovery. *Biochemical Pharmacology*. 2017;134:87-98.
5. World Health Organization. Antimicrobial resistance [Internet]. Geneva: World Health Organization; 2018 [cited 02.20.2018]. Available from: <http://www.who.int/mediacentre/factsheets/fs194/en/>.
6. World Health Organization. Antibiotic resistance [Internet]. Geneva: World Health Organization; 2018 [cited 02.10.2018]. Available from: <http://www.who.int/mediacentre/factsheets/antibiotic-resistance/en/>.
7. Chen DH, Frankel G. Enteropathogenic *Escherichia coli*: unravelling pathogenesis. *FEMS Microbiology reviews*. 2005;29(1):83-98.
8. Kaper JB, Nataro JP, Mobley HL. Pathogenic *Escherichia coli*. *Nature reviews Microbiology*. 2004;2(2):123-40.
9. Sousa CP. The versatile strategies of *Escherichia coli* pathotypes: A mini review. *The Journal of Venomous Animals and Toxins Including Tropical Diseases*. 2006;12(3):363-73.
10. Blackburn CW, McClure PJ. Pathogenic *Escherichia Coli*. *Foodborne Pathogens: Hazards, Risk Analysis and Control*. 2nd ed: CRC Press; 2002.
11. Goering RV, Dockrell HM, Zuckerman M, Riott IM, Chiodini PL. *Mims' Medical Microbiology*. 5th ed: Saunders; 2012.
12. Ocampo PS, Lázár V, Papp B, Arnoldini M, Abel Zur Wiesch P, Busa-Fekete R, et al. Antagonism between bacteriostatic and bactericidal antibiotics is prevalent. *Antimicrobial agents and chemotherapy*. 2014;58(8):4573–82.
13. Silhavy TJ, Kahne D, Walker S. The bacterial cell envelope. *Cold Spring Harbor perspectives in biology*. 2010;2(5):a000414.

14. Rang H, Dale M, Ritter J, Flower R, Henderson G. Rang and Dale's Pharmacology. 7th ed: Churchill Livingstone; 2011.
15. Falagas ME, Kasiakou SK. Colistin: the revival of polymyxins for the management of multidrug-resistant gram-negative bacterial infections. *Clinical infectious diseases*. 2005;40(9):1333-41.
16. Straus SK, Hancock REW. Mode of action of the new antibiotic for Gram-positive pathogens daptomycin: Comparison with cationic antimicrobial peptides and lipopeptides. *Biochim Biophys Acta*. 2006;1758(9):1215-23.
17. Laursen BS, Sorensen HP, Mortensen KK, Sperling-Petersen HU. Initiation of Protein Synthesis in Bacteria. *Microbiology and Molecular Biology Reviews*. 2005;69(1):101-23.
18. Kohanski MA, Dwyer D, Collins J. How antibiotics kill bacteria: from targets to networks. *Nature Reviews Microbiology*. 2010;8(6):423-35.
19. Hooper DC. Mechanisms of fluoroquinolone resistance. *Drug Resistance Updates*. 1999;2(1):38-55.
20. Drlica K, Malik M, Kerns RJ, Zhao X. Quinolone-Mediated Bacterial Death. *Antimicrobial Agents and Chemotherapy*. 2008;52(2):385-92.
21. Norsk legemiddelhåndbok. L1.2.13.1.1 Ciprofloksacin [Internet]. Oslo: Foreningen for utgivelse av Norsk legemiddelhåndbok; 2016 [updated 07.11.2017; cited 01.15.2018]. Available from: <http://legemiddelhandboka.no/Generelle/30452>.
22. Anders B, Nils G. Antibiotikabruk i primærhelsetjenesten: Cystitt [Internet] Oslo: Helsedirektoratet; 2017 [updated 11.11.2017; cited 01.15.2018]. Available from: <http://www.antibiotikaiallmennpraksis.no/index.php?action=showtopic&topic=vXmA4Spa&j=1>.
23. Litleskare I, Blix HS, Rønning M. Antibiotikaforbruk i Norge. *Tidsskrift for Den norske legeforening*. 2008;128(20):2324-9.
24. Munita JM, Arias CA. Mechanisms of Antibiotic Resistance. *Microbiology spectrum*. 2016;4(2).
25. Wise R, Hart T, Cars O, Streulens M, Helmuth R, Huovinen P, et al. Antimicrobial resistance is a major threat to public health. *British Medical Journal*. 1998;317(7159):609-10.
26. Laxminarayan R, Duse A, Wattal C, Zaidi AKM, Wertheim HFL, Sumpradit N, et al. Antibiotic resistance—the need for global solutions. *The Lancet Infectious Diseases*. 2013;13(12):1057-98.

27. Cosgrove SE, Carmeli Y. The impact of antimicrobial resistance on health and economic outcomes. *Clinical Infectious Diseases*. 2003;36(11):1433-7.
28. Norrby R, Powell M, Aronsson B, Monnet DL, Lutsar I, Bocsan IS, et al. The bacterial challenge: time to react - a call to narrow the gap between multidrug-resistant bacteria in the EU and the development of new antibacterial agents. Luxembourg: European Centre for Disease Prevention and Control; 2009.
29. Fernández L, Hancock REW. Adaptive and Mutational Resistance: Role of Porins and Efflux Pumps in Drug Resistance. *Clinical Microbiology Reviews*. 2012;25(4):661-81.
30. Soucy SM, Huang J, Gogarten JP. Horizontal gene transfer: building the web of life. *Nature Reviews Genetics*. 2015;16(8):472-82.
31. Thomas CM, Nielsen KM. Mechanisms of, and Barriers to, Horizontal Gene Transfer between Bacteria. *Nature Reviews Microbiology*. 2005;3(9):711-21.
32. Griffiths AJF. *Modern genetic analysis*. 2nd ed: W.H. Freeman; 1999.
33. Jacoby G. Mechanisms of resistance to quinolones. *Clinical Infectious Diseases*. 2005;41(Suppl 2):120-6.
34. Nikaido H. Multidrug efflux pumps of gram-negative bacteria. *The Journal of Bacteriology*. 1996;178(20):5853-9.
35. Drlica K, Hiasa H, Kerns R, Malik M, Mustaev A, Zhao X. Quinolones: action and resistance updated. *Current Topics in Medicinal Chemistry*. 2009;9(11):981-98.
36. O'Neill J. *Tackling Drug-Resistant Infections Globally: Final report and recommendations*. Washington, D.C.: AMR Review in antimicrobial resistance; 2016.
37. Fischbach MA. Combination therapies for combating antimicrobial resistance. *Current Opinion in Microbiology*. 2011;14(5):519-23.
38. Baym M, Stone L, Kishony R. Multidrug evolutionary strategies to reverse antibiotic resistance. *Science*. 2016;351(6268):aad3292.
39. Szybalski W, Bryson V. Genetic studies on microbial cross resistance to toxic agents. I. Cross resistance of *Escherichia coli* to fifteen antibiotics. *The Journal of Bacteriology*. 1952;64(4):489-99.
40. Pál C, Papp B, Lázár V. Collateral sensitivity of antibiotic-resistant microbes. *Trends in Microbiology*. 2015;23(7):401-7.
41. Imamovic L, Sommer MO. Use of collateral sensitivity networks to design drug cycling protocols that avoid resistance development. *Science translational medicine*. 2013;5(204):204ra132.

42. Podnecky NL, Fredheim EG, Kloos J, Sorum V, Primicerio R, Roberts AP, et al. Conserved collateral susceptibility networks in diverse clinical strains of *Escherichia coli*. bioRxiv. 2018.
43. Lázár V, Pal Singh G, Spohn R, Nagy I, Horváth B, Hrtyan M, et al. Bacterial evolution of antibiotic hypersensitivity. *Molecular Systems Biology*. 2013;9(700).
44. Komp Lindgren P, Karlsson A, Hughes D. Mutation Rate and Evolution of Fluoroquinolone Resistance in *Escherichia coli* Isolates from Patients with Urinary Tract Infections. *Antimicrobial Agents and Chemotherapy*. 2003;47(10):3222-32.
45. Huseby DL, Pietsch F, Brandis G, Garoff L, Tegehall A, Hughes D. Mutation supply and relative fitness shape the genotypes of ciprofloxacin-resistant *Escherichia coli*. *Molecular biology and evolution*. 2017;34(5):1029-39.
46. Kahlmeter G, Poulsen H. Antimicrobial susceptibility of *Escherichia coli* from community-acquired urinary tract infections in Europe: the ECO.SENS study revisited. *International Journal of Antimicrobial Agents*. 2012;39(1):45-51.
47. Bagel S, Hullen V, Wiedemann B, Heisig P. Impact of *gyrA* and *parC* mutations on quinolone resistance, doubling time, and supercoiling degree of *Escherichia coli*. *Antimicrobial Agents and Chemotherapy*. 1999;43(4):868-75.
48. Everett MJ, Jin YF, Ricci V, Piddock LJ. Contributions of individual mechanisms to fluoroquinolone resistance in 36 *Escherichia coli* strains isolated from humans and animals. *Antimicrobial Agents and Chemotherapy*. 1996;40(10):2380-6.
49. Sáenz Y, Zarazaga M, Briñas L, Ruiz-Larrea F, Torres C. Mutations in *gyrA* and *parC* genes in nalidixic acid-resistant *Escherichia coli* strains from food products, humans and animals. *Journal of Antimicrobial Chemotherapy*. 2003;51(4):1001-5.
50. Heisig P. Genetic evidence for a role of *parC* mutations in development of high-level fluoroquinolone resistance in *Escherichia coli*. *Antimicrobial Agents and Chemotherapy*. 1996;40(4):879-85.
51. Lázár V, Nagy I, Spohn R, Csörgő B, Györkei Á, Nyerges Á, et al. Genome-wide analysis captures the determinants of the antibiotic cross-resistance interaction network. *Nature communications*. 2014;5:4352.

Appendices

Appendix A: Results from 1st step static selection of CIP resistant mutants.

Parental isolate	CFU/mL inoculum	CFU/mL mutants	Mutation frequency	Mutant #	Selection concentration CIP ($\mu\text{g/mL}$)	MIC CIP ($\mu\text{g/mL}$)	MIC TMO ($\mu\text{g/mL}$)
K56-2	$1,6 \times 10^9$	10	$6,3 \times 10^{-9}$	1	0,032	0,38	8
	$1,7 \times 10^9$	17	1×10^{-8}	2	0,032	0,25	8
	$1,7 \times 10^9$	17	1×10^{-8}	3	0,032	0,19	8
	$1,7 \times 10^9$	17	1×10^{-8}	4	0,032	0,19	8
	$1,9 \times 10^9$	24	$1,3 \times 10^{-8}$	5	0,032	0,38	6
	$1,9 \times 10^9$	21	$1,1 \times 10^{-8}$	6	0,064	0,25	8
	$1,9 \times 10^9$	21	$1,1 \times 10^{-8}$	7	0,064	0,38	6
	$1,9 \times 10^9$	21	$1,1 \times 10^{-8}$	8	0,064	0,38	8
	$1,6 \times 10^9$	3	$1,9 \times 10^{-9}$	9	0,064	0,25	8
	$1,6 \times 10^9$	3	$1,9 \times 10^{-9}$	10	0,064	0,25	8
K56-12	$2,2 \times 10^9$	20	$9,1 \times 10^{-9}$	1	0,032	0,25	8
	$2,2 \times 10^9$	20	$9,1 \times 10^{-9}$	2	0,032	0,25	8
	$2,2 \times 10^9$	20	$9,1 \times 10^{-9}$	3	0,032	0,25	8
	$1,9 \times 10^9$	20	$1,1 \times 10^{-8}$	4	0,032	0,38	8
	$1,9 \times 10^9$	20	$1,1 \times 10^{-8}$	5	0,032	0,25	8
	$1,9 \times 10^9$	20	$1,1 \times 10^{-8}$	6	0,032	0,5	8
	$2,4 \times 10^9$	30	$1,3 \times 10^{-8}$	7	0,064	0,5	8
	$2,4 \times 10^9$	27	$1,1 \times 10^{-8}$	8	0,128	0,5	12
	$2,4 \times 10^9$	27	$1,1 \times 10^{-8}$	9	0,128	0,5	8
	$2,4 \times 10^9$	27	$1,1 \times 10^{-8}$	10	0,128	0,5	8
K56-78	$2,2 \times 10^9$	55	$2,5 \times 10^{-8}$	1	0,032	0,25	4
	$2,2 \times 10^9$	55	$2,5 \times 10^{-8}$	2	0,032	0,25	4
	$2,2 \times 10^9$	3	$1,4 \times 10^{-9}$	3	0,064	0,38	3
	$2,7 \times 10^9$	24	$8,9 \times 10^{-9}$	4	0,032	0,19	4
	$2,7 \times 10^9$	5	$1,9 \times 10^{-9}$	5	0,064	0,38	3
	$2,7 \times 10^9$	5	$1,9 \times 10^{-9}$	6	0,064	0,38	3
	$3,3 \times 10^9$	21	$6,4 \times 10^{-9}$	7	0,032	0,19	3
	$3,3 \times 10^9$	21	$6,4 \times 10^{-9}$	8	0,032	0,25	4
	$3,3 \times 10^9$	2	$6,1 \times 10^{-10}$	9	0,064	0,38	4
	$3,3 \times 10^9$	2	$6,1 \times 10^{-10}$	10	0,064	0,5	3

Appendix B: MIC values for WT strains.

	K56-2	K56-12	K56-78
MIC CIP (µg/mL)	0,032	0,032	0,032
MIC TMO (µg/mL)	6	8	3

Appendix C: Results from 2nd step static selection of CIP resistant mutants.

Parental isolate	CFU/mL inoculum	CFU/mL mutants	Mutation frequency	Mutant #	Selection concentration CIP (µg/mL)	MIC CIP (µg/mL)	MIC TMO (µg/mL)
K56-2	$1,6 \times 10^9$	≈ 408	$2,6 \times 10^{-7}$	6.1	0,25	2	32
	$1,7 \times 10^9$	≈ 112	$6,6 \times 10^{-8}$	7.1	0,25	1,5	16
	$2,0 \times 10^9$	≈ 320	$1,6 \times 10^{-7}$	8.1	0,25	1,5	24
	$2,0 \times 10^9$	≈ 320	$1,6 \times 10^{-7}$	8.2	0,25	1,5	16
	$2,0 \times 10^9$	≈ 320	$1,6 \times 10^{-7}$	8.3	0,25	1	8
	$1,6 \times 10^9$	≈ 384	$2,4 \times 10^{-7}$	9.1	0,25	1	16
	$1,5 \times 10^9$	≈ 744	5×10^{-7}	10.1	0,5	1,5	24
K56-12	$2,2 \times 10^9$	3	$1,4 \times 10^{-9}$	6.1	0,5	1,5	48
	$2,9 \times 10^9$	TNTC**	-	7.1	0,25	1	24
	$1,5 \times 10^9$	2	$1,3 \times 10^{-9}$	8.1	0,5	1,5	24
	$2,1 \times 10^9$	4	$1,9 \times 10^{-9}$	9.1	0,5	3	32
	$2,5 \times 10^9$	1	4×10^{-10}	10.1	0,5	1,5	48
K56-78	$6,4 \times 10^9$	2	$3,1 \times 10^{-10}$	1.1	0,25	1	64
	$4,2 \times 10^9$	2	$4,8 \times 10^{-10}$	2.1	0,25	1	32
	$5,2 \times 10^9$	16	$3,1 \times 10^{-9}$	3.1	0,5	2	16
	$5,1 \times 10^9$	20	$3,9 \times 10^{-9}$	5.1	0,5	2	12
	$5,1 \times 10^9$	20	$3,9 \times 10^{-9}$	5.2	0,5	2	6
	$2,1 \times 10^9$	24	$1,1 \times 10^{-8}$	5.3	0,5	2	8
	$4,7 \times 10^9$	5	$1,1 \times 10^{-9}$	6.1	0,5	1,5	12
	$1,4 \times 10^9$	17	$1,2 \times 10^{-8}$	6.2	0,5	2	32
	$1,4 \times 10^9$	17	$1,2 \times 10^{-8}$	6.3	0,5	2	24
	$5,5 \times 10^9$	12	$2,2 \times 10^{-9}$	7.1	0,25	1	24
	$4,6 \times 10^9$	8	$1,7 \times 10^{-9}$	9.1	0,5	3	24
	$4,6 \times 10^9$	8	$1,7 \times 10^{-9}$	9.2	0,5	2	24
	$4,8 \times 10^9$	6	$1,3 \times 10^{-9}$	10.1	0,5	3	16
	$2,2 \times 10^9$	18	$8,2 \times 10^{-9}$	10.2	0,5	2	16
	$2,2 \times 10^9$	18	$8,2 \times 10^{-9}$	10.3	0,5	2	32

** Too numerous to count

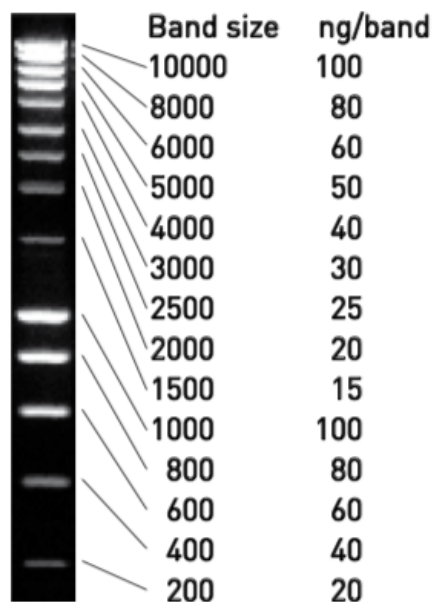
Appendix D: Results from 3rd step static selection of CIP resistant mutants.

Parental isolate	CFU/mL inoculum	CFU/mL mutants	Mutation frequency	Mutant #	Selection concentration CIP (µg/mL)	MIC CIP (µg/mL)	MIC TMO (µg/mL)
K56-2	2,1 × 10 ⁹	2	9,5 × 10 ⁻¹⁰	8.1.1	1	64	2
	2,1 × 10 ⁹	2	9,5 × 10 ⁻¹⁰	8.1.2	1	32	2
	2,7 × 10 ⁹	2	7,4 × 10 ⁻¹⁰	8.2.1	1	96	2
	2,7 × 10 ⁹	2	7,4 × 10 ⁻¹⁰	8.2.2	1	48	2

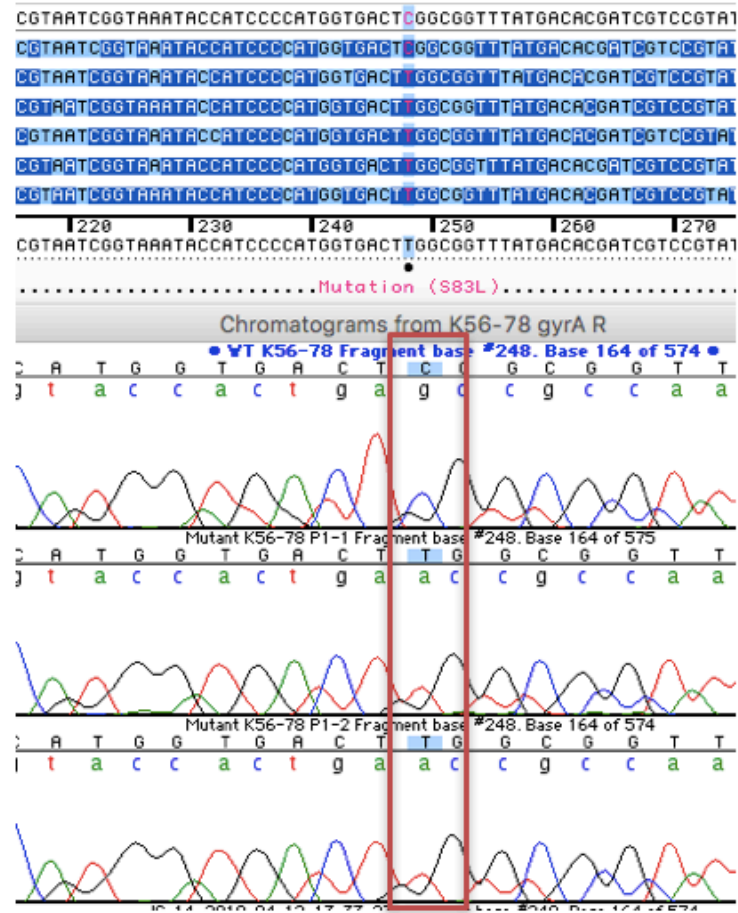
Appendix E: Identified mutations in K56-2 second step mutants statically selected.

Parental isolate	Mutant #	<u>GyrA</u>		<u>ParC</u>	
		Nucleotide mutation	Amino acid mutation	Nucleotide mutation	Amino acid mutation
K56-2	8.1	248 C→T	S83L	-	-
	8.2	248 C→T	S83L	-	-
	8.3	248 C→T	S83L	-	-

Appendix F: SmartLadder MW-1700-10.



Appendix G: Example of identified point mutations in *gyrA* and *parC* by comparison of WT and corresponding mutants.



Appendix H: Expected IC₉₀ values for the control strain (ATCC 25922).

Antimicrobial agent	IC ₉₀ accepted range	EUCAST/CLSI Expected Values
Ceftazidime (CAZ)	0,046875 to 0,5	0,06 to 0,5
Chloramphenicol (CHL)	1,5 to 8	2 to 8
Ciprofloxacin (CIP)	0,003 to 0,016	0,004 to 0,016
Colistin (COL)	0,1875 to 1	0,25 to 1
Gentamicin (GEN)	0,1875 to 1	0,25 to 1
Trimethoprim (TMP)	0,375 to 2	0,5 to 2

Appendix I: Results from IC₉₀ determination of CIP resistant isolates.

Ceftazidime (CAZ)

Parental isolate	Mutant #	Highest concentration tested (µg/mL)	IC ₉₀	Fold change
K56-2	WT	0,5	0,09375	
	P1-1	0,5	0,09375	0
	P1-2	0,5	0,125	1,33
	P2-1	0,5	0,1875	2
	P2-2	0,5	0,125	1,33
	P2-3	0,5	0,09375	0
K56-12	WT	0,5	0,125	
	P1-1	0,5	0,125	0
	P2-2	0,5	0,125	0
K56-78	WT	0,5	0,09375	
	P2-1	0,5	0,09375	0
	P2-2	0,5	0,125	1,33
	P2-3	0,5	0,125	1,33

Chloramphenicol (CHL)

Parental isolate	Mutant #	Highest concentration tested (µg/mL)	IC ₉₀	Fold change
K56-2	WT	16	4	
	P1-1	16	4	0
	P1-2	16	4	0
	P2-1	16	6	1,5
	P2-2	16	4	0
	P2-3	16	4	0
K56-12	WT	16	6	
	P1-1	16	6	0
	P2-2	16	6	0
K56-78	WT	16	6	
	P2-1	16	6	0
	P2-2	16	8	1,33
	P2-3	16	6	0

Ciprofloxacin (CIP)

Parental isolate	Mutant #	Highest concentration tested (µg/mL)	IC ₉₀	Fold change
K56-2	WT	0,0625	0,012	
	P1-1	16	1	83,3
	P1-2	16	1,5	125
	P2-1	4	1	83,3
	P2-2	16	6	500
	P2-3	4	0,75	62,5
K56-12	WT	0,0625	0,012	
	P1-1	4	0,75	62,5
	P2-2	4	0,75	62,5
K56-78	WT	0,0625	0,012	
	P2-1	4	0,5	41,7
	P2-2	4	0,5	41,7
	P2-3	4	0,5	41,7

Colistin (COL)

Parental isolate	Mutant #	Highest concentration tested (µg/mL)	IC ₉₀	Fold change
K56-2	WT	2	0,5	
	P1-1	2	0,5	0
	P1-2	2	0,375	-1,33
	P2-1	2	0,5	0
	P2-2	2	0,75	1,5
	P2-3	2	0,5	0
K56-12	WT	2	0,375	
	P1-1	2	0,5	1,33
	P2-2	2	0,5	1,33
K56-78	WT	2	0,5	
	P2-1	2	0,5	0
	P2-2	2	0,5	0
	P2-3	2	0,5	0

Gentamicin (GEN)

Parental isolate	Mutant #	Highest concentration tested (µg/mL)	IC ₉₀	Fold change
K56-2	WT	2	0,375	
	P1-1	2	0,25	-1,5
	P1-2	2	0,375	0
	P2-1	2	0,25	-1,5
	P2-2	2	0,1875	-2
	P2-3	2	0,1875	-2
K56-12	WT	2	0,375	
	P1-1	2	0,375	0
	P2-2	2	0,5	1,33
K56-78	WT	1	0,25	
	P2-1	1	0,125	-2
	P2-2	1	0,1875	-1,33
	P2-3	1	0,25	0

Trimethoprim (TMP)

Parental isolate	Mutant #	Highest concentration tested ($\mu\text{g/mL}$)	IC₉₀	Fold change
K56-2	WT	2	0,25	
	P1-1	2	0,25	0
	P1-2	2	0,25	0
	P2-1	2	0,1875	-1,33
	P2-2	2	0,25	0
	P2-3	2	0,25	0
K56-12	WT	2	0,5	
	P1-1	2	0,375	-1,33
	P2-2	2	0,375	-1,33
K56-78	WT	2	0,5	
	P2-1	2	0,375	-1,33
	P2-2	2	0,5	0
	P2-3	2	0,375	-1,33

